Statistical approaches for the definition of landslide rainfall thresholds and their uncertainty using rain gauge and satellite data

M. Rossi[a,b,*], S. Luciani[a,b], D. Valigi[b], D. Kirschbaum[c], M.T. Brunetti[a,b], S. Peruccacci[a], and F. Guzzetti[a]

[a] Consiglio Nazionale delle Ricerche, Istituto di Ricerca per la Protezione Idrogeologica, Perugia, Italy

[b] Dipartimento di Fisica e Geologia, Università degli Studi di Perugia, via A. Pascoli, s.n.c. 06123, Perugia, Italy

[c] NASA Goddard Space Flight Center, Hydrological Sciences Laboratory, Greenbelt, Md., Unites States

* Corresponding author. Tel: 0039 075 5014421; Fax: 0039 075 5014420.

E-mail address: mauro.rossi@irpi.cnr.it (M. Rossi)

Abstract

Models for forecasting rainfall-induced landslides are mostly based on the identification of empirical rainfall thresholds obtained exploiting rain gauge data. Despite their increased availability, satellite rainfall estimates are scarcely used for this purpose. Satellite data should be useful in ungauged and remote areas, or should provide a significant spatial and temporal reference in gauged areas. In this paper, the analysis of the reliability of rainfall thresholds based on rainfall remote sensed and rain gauge data for the prediction of landslide occurrence is carried out. To date, the estimation of the uncertainty associated with the empirical rainfall thresholds is mostly based on a bootstrap resampling of the rainfall duration and the cumulated event rainfall pairs (*D,E*) characterizing rainfall events responsible for past failures. This estimation does not consider the measurement uncertainty associated with *D* and *E*. In the paper, we propose (i) a new automated procedure to reconstruct *ED* conditions responsible for the landslide triggering and their uncertainties, and (ii) three new methods to identify rainfall threshold for the possible landslide occurrence, exploiting rain gauge and satellite data. In particular, the proposed methods are based on least square (LS), quantile regression (QR) and nonlinear least square (NLS) statistical approaches. We applied the new procedure and methods to define empirical rainfall thresholds and their associated uncertainties in the Umbria region (central Italy) using both rain-gauge measurements and satellite estimates. We finally validated the thresholds and tested the effectiveness of the different threshold definition methods with independent landslide information. The NLS method among the others performed better in calculating thresholds in the full range of rainfall durations. We found that the thresholds obtained from satellite data are lower than those obtained from rain gauge measurements. This is in agreement with the literature, where satellite rainfall data underestimate the "ground" rainfall registered by rain gauges.

Key words: Landslide prediction; Rainfall threshold; Satellite rainfall estimates; Threshold uncertainty

1. Introduction

Prediction of landslide occurrence in widespread areas relies on the definition of empirical rainfall thresholds, which are defined through the analysis of past rainfall events that have resulted in slope failures. In Italy, every year landslides initiated by intense or prolonged rainfall produce casualties and economic damages (Salvati et al., 2010, 2013). In this country and elsewhere, forecasting rainfall-induced landslides, and determining the rainfall conditions responsible for the initiation of landslides remain a difficult task (Tabios and Salas, 1985; Morrissey et al., 1995; Aleotti and Chowdhury, 1999; Aleotti, 2004; Guzzetti et al., 2007, 2008; Frattini et al., 2009; Jaiswal and van Westen, 2009; Penna et al., 2011; Verworn and Haberlandt, 2011; Berti et al., 2012; Peruccacci et al., 2012; Staley et al., 2013; Marra et al., 2014; Melillo et al., 2014; Vessia et al., 2014). Rainfall is measured on the ground using rain gauges, or estimated by combining information captured by multiple satellite sensors. Rainfall (ground) measurements or (remote) estimates can be used to predict the possible occurrence of landslides in an area. While ground rainfall data are commonly used for the prediction of landslides (Guzzetti et al., 2007), only few studies show how satellite remote estimates can be used for landslide prediction over large areas (Kirschbaum et al., 2012). Moreover, satellite data should be particularly useful substituting traditional ground based measurements in ungauged and remote areas, while may provide a significant spatial and temporal reference in gauged areas.

A large and growing body of literature has investigated the use of empirical rainfall thresholds to forecast rainfall-induced landslides, particularly over large areas. The most common types of thresholds are rainfall mean intensity (*I*) – rainfall duration (*D*) thresholds (Caine, 1980; Innes, 1983; Crosta and Frattini, 2001; Aleotti, 2004; Guzzetti et al., 2007; Dahal and Hasegawa, 2008;

Guzzetti et al., 2008; Brunetti et al., 2010; Saito et al., 2010; Staley et al., 2013; Nikolopoulos et al., 2014; Segoni et al., 2014) or cumulated event rainfall (*E*) – rainfall duration (*D*) thresholds (Innes, 1983; Guzzetti et al., 2007; Floris and Bozzano, 2008; Li et al., 2011; Peruccacci et al., 2012). In Italy, rainfall thresholds for possible landslide occurrence were defined for geographical areas of different extent, including national (Brunetti et al., 2010), regional (Ceriani et al., 1992; Calcaterra et al., 2000; Crosta and Frattini, 2001; Aleotti, 2004; Segoni et al., 2009; Brunetti et al., 2010; Tiranti and Rabuffetti, 2010; Berti et al., 2012; Martelloni et al., 2012; Peruccacci et al., 2012; Lazzari et al., 2013; Gariano et al., 2014; Melillo et al., 2014; Vennari et al., 2014), and local thresholds (Guadagno, 1991; Bolley and Oliaro, 1999; Deganutti et al., 2000; Biafore et al., 2001; Marchi et al., 2002; Giannecchini, 2005; Cevasco et al., 2010; Giannecchini et al., 2012; Rosi et al., 2012).

For wide and diversified study areas, rainfall thresholds are still the most appropriate and largely used approach for landslide forecasting. Conversely, physically based models requires measuring/collecting all the environmental, geotechnical, hydrological (and possible other) parameters and they can be applied reasonably to small areas (at hillslope or small basin scale). Previous studies, in a larger and partially overlapped study area and hence in similar geo-environmental conditions, analysed the dependence of rainfall thresholds on the lithology (Peruccacci et al., 2012). The authors conclude that only marginally lithological conditions affect rainfall thresholds and they suggest that a minimum number of 175 landslide events is required to limit the rainfall threshold uncertainty below 10%. This kind of investigation was not performed in this paper, given the limited amount of landslide information (187 rainfall-induced landslides) available in the period 2002–2010 in the selected study area, corresponding to the Umbria region (central Italy) extending for about 8,460 km^2.

The main objective of this paper is to provide a new statistical procedure for (i) the identification of rainfall events responsible for slope failures and (ii) the definition of rainfall thresholds and their associated uncertainty using rain gauge measurements and satellite rainfall estimates and information on landslide occurrence. The proposed procedure is entirely automated and integrates a new statistical approach to define the rainfall threshold parameter uncertainty. Such approach relies upon the uncertainty of rainfall data, as opposed to the resampling approaches for the uncertainty estimation proposed so far in the literature (i.e. Peruccacci et al., 2012). The thresholds obtained reconstructing the rainfall events with the "automated procedure" are compared with those obtained using the so-called "expert method" (Brunetti et al. 2010). For this purpose, we exploit for the same period: (i) ground-based rainfall measurements obtained by a network of 60 rain gauges, and (ii) satellite rainfall estimates provided by NASA's Tropical Rainfall Measuring Mission (TRMM) Multi-satellite Precipitation Analysis (TMPA) covering an area from 50ºN to 50ºS, with a 0.25° × 0.25° spatial resolution. Although TRMM stopped providing data in April, 2015, the TMPA product continues to be run and is projected to carry on through early 2017. We did not consider NASA's Global Precipitation Measurement (GPM) mission derived rainfall products because currently these data are not available prior to 2014 (Huffman et al., 2013).

Separate *ED* thresholds for the possible occurrence of rainfall-induced landslides in the study area are determined from rainfall duration and cumulated event rainfall conditions derived from rain gauge measurements and satellite estimates, using three different statistical methods. The thresholds obtained for the different rainfall datasets using the three different statistical approaches are compared, their validation performances are evaluated, and their possible use to forecast landslide occurrence is discussed.

This paper is organized as follows. After a brief description of the study area (Section 2), we present the landslide information and the rainfall data available to us (Section 3). Next, we use a manual and an automated procedure to determine *ED* conditions that have resulted in landslides and the associated uncertainties (Section 4). Next, using the different sets of (*D*,*E*) pairs obtained from the rain gauge measurements and the satellite rainfall estimates; we test three different methods to determine *ED* rainfall thresholds, their uncertainties and their validation performances (Section 5). Then we discuss the results obtained, and specifically the advantages and the limitations of the three methods (Section 6). We conclude (Section 7) summarizing the main lessons learnt.

2. Study area

We performed our study in the Umbria region that extends for 8,456 km^2 in central Italy (**Fig. 1**). In the study area, landscape is hilly or mountainous, with large valleys and intra mountain basins drained by the Tiber River and its tributaries. Elevation in the area averages 500 m a.s.l., and ranges from 50 to 2478 m a.s.l., at Monte Vettore. Climate is Mediterranean and rainfall falls mostly from October to December and from March to May. Five groups of rock types crop out in Umbria (**Fig. 1**), including carbonate rocks (CC), flysch deposits (FD), volcanic rocks (VR), a chaotic complex (CH), and post-orogenic sediments (PO). Each lithological group comprises different rock types varying in strength from hard to weak and soft rocks. Post-orogenic sediments include continental and marine clay, silt, sand, gravel, and travertine. Flysch deposits comprise well-stratified and graded marl, sandy shale, and mud orderly interbedded with greywacke's, coarse and fine sandstone, calcarenite, and gypsum deposits. Carbonate rocks comprise massive and layered limestone, chert, marl, and shale. The chaotic complex is a mélange of clay, shale, marl, sandstone, and calcarenite, and the volcanic complex includes lava flows, ignimbrites, and pyroclastic deposits (Guzzetti et al., 1996). Landslides are frequent and abundant in Umbria (Guzzetti et al., 1996, 2003) and are caused primarily by intense or prolonged rainfall (Cardinali et al., 2006; Peruccacci et al., 2012). Subordinately, slope failures are triggered by rapid snowmelt (Cardinali et al., 2000) and earthquakes (Esposito et al., 2000; Antonini et al., 2002). Landslides in Umbria are most abundant in forested and cultivated areas. In forested areas, landslides are mostly old and very old, while in cultivated areas old and very old landslides coexist with recent and active slope failures (Torri et al., 2006).

3. Data

3.1. Landslides

We selected two independent datasets of rainfall-induced landslides in the Umbria region. The first dataset includes 170 data from the national catalogue of rainfall events that triggered landslides in Italy in the period 2002–2009 (Brunetti et al., 2010). We added 17 new events to the catalogue searching new information, and obtaining a total of 187 landslides in the period 2002–2010 (yellow circles in **Fig. 2A**). We searched information on rainfall-induced landslides in national, regional, and local newspapers, and in reports of the local fire brigades. For each landslide, data listed in the catalogue include: (i) the date and the known or inferred time of the landslide occurrence (the latter if available), (ii) its geographical location, and (iii) the type of the failure, adopting the landslide classification proposed by Cruden and Varnes (1996).

Additionally, the dataset reports information on the uncertainty associated with the temporal and spatial identification of landslides. This first dataset was used for the reconstruction of the rainfall conditions responsible for landslides and then used for the calibration of the *ED* rainfall thresholds for the possible landslide occurrence proposed in this work. The second dataset, provided by the Umbria Functional Centre (UFC) of the Civil Protection Department, was used to validate the rainfall thresholds and the criteria/methods used to define the thresholds. This second dataset consists of 192 events at daily scale, that triggered rainfall-induced landslides in the Umbria region during the same period covered by the first dataset (orange circles in **Fig. 2A**). For this second landslide dataset, we have a limited knowledge on (i) the spatial and temporal accuracy of the collected information and (ii) the criteria used for the inventory collection.

3.2. Rainfall

Two independent sources of rainfall information were available to us. The first consisted of hourly rainfall measurements obtained by a network of 60 rain gauges in Umbria (**Fig. 2B**). This is part of a larger network of more than 2000 rain gauges in Italy managed by the Italian National Civil Protection Department and the regional governments. The second source of rainfall information consisted of satellite rainfall estimate products provided by the NASA Tropical Rainfall Measuring Mission (TRMM), Multi-satellite Precipitation Analysis (TMPA), TRMM version 6 (V6) 3B42.

We decided to use the TRMM version 6 instead the last available TRMM version (TMPA-V7 and TMPA-V7 Real Time (R-T) following the analysis performed by Rossi et al. (submitted). They found that the new TRMM rainfall estimates are closer to the data measured by rain gauges, but they exhibit the lowest determination coefficients and the largest estimation variability compared to the TMPA-V6 and TMPA-V6-RT. This reflects in a simpler scaling/tuning process when using the older products. Moreover, Rossi et al. (submitted) suggest that rainfall events derived exploiting an automated procedure, using the different satellite rainfall data types, are statistically different as well as their spatial arrangements and patterns across the Italian territory. In particular, the new TRMM products TMPA-V7 and TMPA-V7-RT, compared to TMPA-V6 and TMPA-V6-RT, failed to capture the dependence/conditioning given by the morphology identified by the rain gauge data. Finally, between the two TMPA-V6 product versions, we decided to use the research product rather than real-time, mainly because this incorporates gauge calibration.

The TMPA-V6 product covers an area from 50ºN to 50ºS, with a 0.25° × 0.25° spatial resolution, and a 3-hours temporal resolution (Huffman et al., 2007, 2010). This product merges high-quality microwave and infrared precipitation estimates after calibration to the combined TRMM Precipitation Radar (PR) and TRMM Microwave Imager (TMI) precipitation product from the TRMM satellite, and factors in monthly precipitation gauge analyses to create the 3-hourly product. In the analysis, we select the rainfall data series corresponding to the 13 TRMM pixel centroids inside the Umbria regional boundary (**Fig. 2B**). For this study, we used rain gauge data and satellite rainfall estimates in the period from 2002 to 2010.

4. Rainfall conditions responsible for landslides

In order to determine the rainfall responsible for a landslide, the identification of the rainfall start time and the information on the landslide occurrence time are required (Aleotti, 2004; Guzzetti et al., 2007; Brunetti et al., 2010; Saito et al., 2010; Shamsudin et al., 2010, Berti et al., 2012; Peruccacci et al., 2012; Rossi et al. 2012; Staley et al., 2013; Melillo et al., 2014; Nikolopoulos et al., 2014; Vessia et al., 2014). This task is not trivial and it is characterized by uncertainty (Aleotti, 2004; Godt et al., 2006; Guzzetti et al., 2008; Bach-Kirschbaum et al., 2012). For a rainfall event responsible for a landslide, D was determined by measuring the time between the moment, or period, of initiation of the failure(s) (rainfall end time, T_e) and the time when the rainfall event started (rainfall start time, T_s), i.e. $D = T_e - T_s$ (Brunetti et al., 2010; Rossi et al., 2012; Rossi et al., 2013; Rossi et al., 2014; Vessia et al., 2014). Generally, T_e depends on the temporal accuracy associated with each landslide information (Brunetti et al., 2010). For landslides that failed after the end of the rainfall event, T_e is taken to coincide with the end of the rainfall event. Precise identification of T_s was often problematic. A dry period between two successive rainfall values is required to separate different rainfall events. A dry period is a period without rainfall, or with rainfall below a minimum threshold level. In this work, we adopted two independent procedures to separate rainfall events and to determine rainfall conditions presumably responsible for the landslide occurrence. Both procedures used the same information i.e., (i) the catalogue of rainfall events with landslides in Umbria, (ii) the hourly rainfall measurements, and (iii) the TRMM satellite rainfall estimates. The first procedure, commonly used in literature (Brunetti et al., 2010; Peruccacci et al., 2012; Vennari et al., 2014) to reconstruct rainfall events with landslides and named "expert method", is manual and heuristic and it is used here as a benchmark. The second procedure, i.e. the "automated procedure" introduced in this work is automatic (i.e. coded in R; R Core Team, 2015) and objective (Rossi et al., 2012).

4.1. Expert method

The manual procedure started with the selection of a single rain gauge according to: (i) the geographic distance to the landslide, not exceeding 15 km from the landslide, (ii) the elevation of the rain gauge, comparable to the elevation of the slope failure, and (iii) the location of the rain gauge with respect to the local topographical and morphological settings (Brunetti et al., 2010; Peruccacci et al., 2012; Vessia et al., 2014). For the satellite-based rainfall estimates, the centroid of each grid cell was considered a hypothetical ("virtual") rain gauge, and the centroids closest to the landslides were selected. When the representative rain gauge or satellite centroid was identified, D (in hour), and E (in mm) were calculated. As aforementioned, the selection of T_s is difficult, particularly when the rainfall is not continuous. To account for different meteorological regimes, Brunetti et al. (2010) considered a two-day (48 h) period without rainfall to separate rainfall events during the period May–September, and a four-day (96 h) period between October and April. to identify rainfall events with landslides in Italy. In this analysis, we used the same settings. **Fig. 3** shows the rainfall conditions selected exploiting the expert method, and calculated using rain gauge measurements (red dots in **Fig. 3A**) and satellite rainfall estimates (green dots in **Fig. 3B**), respectively.

4.2. Automated procedure

The first step in the automated procedure was the selection of a pool of rain gauges, or satellite rainfall centroids, considered representative of the rainfall responsible for each landslide in the catalogue. We chose a minimum of seven and a maximum of 12 rain gauges for each landslide. The representative rain gauges were selected within a planimetric distance of 10 km, and within an elevation range of 100 m, from the geographical location of the landslide. If an insufficient number of rain gauges were found in the selected distance and elevation boundaries, the procedure increased progressively the search distance of 0.1 km step, and the elevation range of 5 m step, to reach the requested minimum of seven rain gauges (R_i, i = 1,…,7; **Fig. 4**). Satellite centroids were selected using solely the planimetric distance of 10 km from the landslide. If an insufficient number of centroids were found, the procedure increased progressively the search distance of 0.1 km step until a minimum of centroids was selected (S_i, I = 1,…,4; **Fig. 4**).

The second step of the automated procedure was the identification of the rainfall conditions responsible for the landslides in the catalogue as proposed by Rossi et al. (2012, 2013, 2014). As for the expert method, the procedure needs to identify T_e and T_s. In this work, we used a dry separation period of 72h (Rossi et al., 2013, 2014), and two minimum rainfall levels of 0.2 mm and of 0.0 mm for the rain gauge measurements and the TRMM satellite rainfall estimates, respectively.

The last step of the automated procedure was the determination of D and E of the rainfall events responsible for each landslide in the catalogue, reconstructed using the representative rain gauges and centroids. For each landslide, multiple (D,E) pairs that probably have resulted in slope instability were determined. For D and E, we calculated the median (D_{50} and E_{50}), the 1st quantile (D_{25} and E_{25}), and the 3rd quartile (D_{75} and E_{75}). We assumed that the quantities $D_{75} - D_{25}$ and $E_{75} - E_{25}$ represent the uncertainty associated with D and E, respectively. Thus in the DE plane, rainfall conditions associated with landslides can be any pair in the rectangle identified by the two uncertainties. The ED rainfall conditions characterized by large uncertainties were excluded from the analysis. In particular, if the following conditions (**Eqs. 1 and 2**) are contemporarily verified, the event is characterized by a large uncertainty, and hence discarded from the analysis:

$$E_{50} - \frac{E_{50}}{2} < E_{25} \quad \text{and} \quad E_{75} > E_{50} + \frac{E_{50}}{2} \tag{1}$$

$$D_{50} - \frac{D_{50}}{2} < D_{25} \quad \text{and} \quad D_{75} > D_{50} + \frac{D_{50}}{2} \tag{2}$$

Fig. 5 shows the (D_{50},E_{50}) rainfall conditions and their associated uncertainties selected exploiting the aforementioned procedure, and calculated using rain gauge measurements (red dots in **Fig. 5A**) and satellite rainfall estimates (green dots in **Fig. 5B**). The automated procedure allows the estimation of the uncertainty associated with the rainfall conditions that have probably resulted in landslides (**Fig. 5**). We maintain that this is an advantage over the expert method which identifies a single *ED* rainfall condition responsible for the slope instability (**Fig. 3**).

5. Definition of rainfall thresholds

We used the empirical rainfall data (rainfall measurements from rain gauges and rainfall estimates from satellite) reconstructed with the expert method (**Fig. 3**) and data reconstructed with the automated procedure (**Fig. 5**) to determine rainfall thresholds for possible landslide occurrence in Umbria.

For rainfall conditions reconstructed with the expert method, we defined rainfall thresholds using the frequentist method proposed by Brunetti et al. (2010) and modified by Peruccacci et al. (2012). Thresholds are power law curves of the form:

$$E = (\alpha \pm \Delta\alpha) D^{(\gamma \pm \Delta\gamma)} \tag{3}$$

where *E* is the cumulated (total) event rainfall (in mm), *D* is the duration of the rainfall event (in h), α is a scaling parameter (the intercept), γ is the slope of the power law threshold curve, and $\Delta\alpha$ and $\Delta\gamma$ are the uncertainties associated with α and γ, respectively. The method allows defining thresholds at different non-exceedance probability levels and adopts a "bootstrap" non-parametric statistical technique (Efron, 1979; Efron and Tibshirani, 1994) to estimate the uncertainty associated with the threshold curve. **Fig. 6** shows frequentist thresholds (*F*) at 5% non-exceedance probability obtained exploiting rainfall conditions reconstructed with the expert method using rain gauges (**Fig. 3A**) and satellite estimates (**Fig. 3B**). **Table 1** lists the relative threshold parameters defined with the frequentist method.

For rainfall conditions obtained by the automated procedure we proposed and tested three new methods to define empirical rainfall thresholds. These new three methods allow to account for the uncertainty associated with *D* and *E*. The three methods include (i) a Least Square (LS) method (i.e. similar to the statistical approach used in F), (ii) a Quantile Regression (QR) method, and (iii) and a Nonlinear Least Square (NLS) method. These methods allow propagating the uncertainty associated with the *ED* rainfall conditions responsible for landslides to the thresholds. Conversely, the uncertainty of thresholds defined with the frequentist method applied to the rainfall conditions reconstructed with the expert method is obtained using a bootstrap resampling approach.

To account for the uncertainty associated with *D* and *E* in the calculation of the rainfall thresholds, we used a specific statistical procedure. Starting from the empirical data set of *n* events, we generated 10,000 samples of *n* randomly selected events. For each sample, the synthetic values of *D* and *E* were sampled from their uncertainty ranges using a uniform distribution. We applied separately the three methods to define the rainfall thresholds and their associated uncertainties. The significance levels of threshold parameters, obtained using the different statistical approaches, were estimated from the *t*-test statistics and corresponding (two-sided) *p*-values (R Core Team, 2015).

5.1. Least Square method (LS)

The Least Square method (Wilkinson and Rogers, 1973; Chambers, 1992) consists of fitting each of the 10,000 synthetic samples with a power law curve:

$$E = \alpha D^{\gamma} \qquad \text{Eq. (4)}$$

The probability density distributions of α and γ parameters obtained from the 10,000 power law curves were calculated, and their median values $\hat{\alpha}$ and $\hat{\gamma}$ were chosen as the best LS fit. Next, we estimated the uncertainty associated with the fit defining α_{inf} and γ_{inf} as the 5th percentile and α_{sup} and γ_{sup} as 95th percentile of the two distributions. Then, for each (D_{50},E_{50}) pair, we calculated the difference between E_{50} and the corresponding value on the LS fit (i.e., the fit residuals). Lastly, we calculated the probability density function of the residuals, allowing us to define thresholds for different non-exceedance probability levels (Brunetti et al., 2010). **Fig. 7A,B** shows the LS thresholds, and their uncertainties at 5% non-exceedance probability for the ground-based rain gauge measurements (**Fig. 7A**) and for the TRMM satellite rainfall estimates (**Fig. 7B**). **Table 2** lists the parameters of the power law thresholds obtained using the LS model and their associated significance levels.

Visual inspection of **Fig. 7A,B** reveals that the LS threshold captured reasonably well the general trend of the cloud of the empirical (*D,E*) data, but failed to catch a part the distribution of the empirical data, particularly at durations less than about 50 h and higher than about 400 h. In an attempt to overcome the problem, we used a different threshold curve based on a Quantile Regression approach (Koenker and Bassett, 1978).

5.2. Quantile Regression (QR)

Quantile Regression was introduced in the 1970s as an extension to the classical linear regression model (Koenker and Bassett, 1978). Classical linear regression minimizes the sums of the squared residuals enabling us to estimate a model for conditional mean functions. Similarly, QR minimizes asymmetrically the weighted absolute residuals. This provides a way for estimating models for the conditional median functions (50th percentile), and for any other conditional quantile functions.

In this work, we performed a QR for the 5th percentile, to define an empirical threshold at 5% non-exceedance probability level, for each of the 10,000 synthetic samples using the power law in **Eq. (4)**. Next, adopting the same approach used for the LS method, we calculated the empirical probability density distributions of α and γ for the 10,000 power law curves, and we selected their median values $\hat{\alpha}$ and $\hat{\gamma}$ to represent the best QR model. Lastly, we estimated the uncertainty associated with the QR model by selecting α_{inf} and γ_{inf} as the 5th percentile and α_{sup} and γ_{sup} as the 95$^{\mathrm{th}}$ percentile of the two distributions. **Fig. 7C,D** shows the QR thresholds and their uncertainties at 5% non-exceedance probability, for the rain gauge measurements (**Fig. 7C**) and for the TRMM satellite rainfall estimates (**Fig. 7D**). **Table 2** lists the parameters of the power law thresholds calculated using the QR models and their associated significance levels.

Fig. 7C,D shows that the QR threshold fitted reasonably well the lowest empirical (*D,E*) data for durations larger than about 12 h. For shorter durations, the QR threshold underestimates significantly the amount of rainfall required to initiate a landslide. The underestimation is a result of the reduced number of empirical data points for D < 12 h. The underestimation may result in an excessive number of false alarms (Brunetti et al., 2010; Tiranti and Rabuffetti, 2010; Berti et al., 2012; Martelloni et al., 2012; Lagomarsino et al., 2013; Staley et al., 2013; Nikolopoulos et al., 2014; Segoni et al., 2014). In order to overcome this problem, we experimented a nonlinear threshold model based on a least-square approach.

5.3. Nonlinear Least Square model (NLS)

The power law thresholds calculated using the LS and the QR models, resulted inadequate because they poorly bordered the lowest empirical data, as shown in **Fig. 7A–D**. Therefore, we adopted a three-parameter power-law threshold model, similar to the threshold model proposed by Cannon and Ellen (1985),

$$E = t + \alpha D^{\gamma} \qquad \text{Eq. (5)}$$

Where t, α and γ are the threshold parameters. We estimated the three model parameters in the linear coordinates using a Nonlinear (weighted) Least Square estimation approach (Bates and Watts, 1988). For consistency with the previous methods, the NLS thresholds were defined at 5% non-exceedance probability level. Adopting the same approach used for the previous models, we calculated the empirical probability density distributions of the model parameters (t, α, γ) for the 10,000 NLS curves obtained from the synthetic samples. In particular, for each of 10,000 synthetic samples, we estimated the 5th percentiles of D and E, in a mobile kernel window moved along the duration axis (i.e. along x-axis in **Fig. 7**), starting from the (D,E) pair with lowest duration value to the pair with the highest one. To define the kernel window size we tested two different approaches using: (i) a fixed window size, and (ii) a variable window size containing a fixed number of (D,E) pairs. We repeated the threshold calculation exploiting these two approaches using different kernel window sizes and different number of points. Best performances were obtained using a variable window size with 10 pairs. The (*D*,*E*) pairs (corresponding to the 5^{th} percentiles) obtained for each synthetic sample were then fitted using the NLS method to estimate the three threshold curve parameters (**Eq. 5**). **Table 2** lists the parameters for the power law NLS thresholds and their associated significance levels, while **Fig 7E,F** show the NLS curves and their uncertainties, for the rain gauge measurements (**Fig. 7E**) and for the TRMM satellite rainfall estimates (**Fig. 7F**). Inspection of **Fig. 7E,F** reveals that the NLS threshold models fitted adequately the lowest values of the empirical data distribution, for the entire duration range. This result was obtained at the expense of a larger uncertainty for the events with $D < 12$ h (**Fig. 7E,F**). **Fig. 8** shows the comparison of the thresholds obtained for the rain gauge measurements (**Fig. 8A**) and for the satellite estimates (**Fig. 8B**), with the "frequentist expert method" and the three models proposed in this paper (LS, QR, NLS).

5.4. Threshold methods validation

A second independent dataset of rainfall-induced landslides in Umbria region provided by the Umbria Functional Centre (UFC) was used (i) to validate/test the effectiveness of the thresholds defined using satellite and rain gauge data in forecasting new landslides, (ii) to test the effectiveness of the methods to derive rainfall thresholds for the possible landslide occurrence.

To address the first issue, we compared the thresholds defined using different methods (coloured lines in **Fig. 9**), with rainfall conditions triggering landslides (red dots in **Fig. 9 A,B**) reconstructed from the independent UFC dataset (i.e. not used in the rainfall threshold identification). Rainfall conditions were derived using the automated procedure proposed in Section 4.2 using rain gauge measurements (**Fig. 9A**) and satellite rainfall estimates (**Fig. 9B**).

Table 3 summarizes the number and percentage of UFC rainfall conditions triggering landslides below the different thresholds derived for rain gauge and satellite rainfall data.

To test the effectiveness of the methods proposed in this work to derive rainfall thresholds for the possible landslide occurrence, we applied them using the independent UFC landslide dataset. For this purpose we first reconstructed rainfall conditions (from satellite and rain gauge data) responsible for landslides occurrence using the automated procedure described in Section 4.2, and then defined new rainfall thresholds using the different methods described in Sections 5.1, 5.2 and 5.3. Table 4 summarizes the *ED* rainfall threshold parameters estimated for the Umbria region for a non-exceedance probability of 5%, and using a period of 72 h without rain to separate two rainfall events.

6. Results and discussion

The performed analysis compared the use of rainfall gauge measurements and satellite estimates for determining *ED* thresholds for possible landslide occurrence, exploiting two different methods: (i) expert method and (ii) automated procedure.

The log-log plots of the empirical (*D,E*) data points obtained by the expert method show that the majority of the landslides (77%) listed in the catalogue in Umbria (Section 3.1) were caused by precipitation characterized by long durations and low mean rainfall intensities. The remaining landslides (23%) were triggered by rainfall characterized by short duration and high rainfall rates. In particular, in the dry period from May to September, rainfall events with $D < 24$ h (58%) predominate, whereas in the wet period between October and April rainfall events with $D > 24$ h (78%) are most abundant. Furthermore, comparing Fig. 3A with Fig. 3B, it can be seen that rainfall events reconstructed using TRMM satellite estimates were characterized by a lower cumulated rainfall E than the corresponding events reconstructed using rain gauge measurements. This is in agreement with other comparison of TRMM estimates and gauge data in Italy (Rossi et al., 2012, submitted).

We have derived the empirical rainfall thresholds from the two data sets shown in **Fig. 6** considering a non-exceedance probability of 5%, and estimating the uncertainty associated with the thresholds as proposed by Brunetti et al. (2010), and improved by Peruccacci et al. (2012). To evaluate the statistical uncertainty associated with the two parameters γ and α of **Eq. (3)**, we used a bootstrapping technique (Peruccacci et al., 2012). The shaded areas around the threshold lines show that uncertainty associated with the thresholds increases with the rainfall duration.

Table 1 reveals that the underestimation of the satellite rainfall estimates is clearly reflected in the rainfall thresholds. The values of α for satellite rainfall threshold are lower than those obtained for the rain gauge rainfall threshold while the values of γ are very similar. Therefore, the rainfall thresholds are approximately parallel to each other with the satellite threshold moved downwards.

The expert method is time consuming and error prone, and the quality of the results obtained depends on the experience and consistency of the investigator (Melillo et al., 2014) and do not include the uncertainties of rainfall data (**Fig. 3**). This aspect was considered by the automated procedure where, a pool of rain gauges or satellite rainfall centroids was selected for each landslide. Thus, for each landslide in the catalogue, multiple reconstructions of the rainfall conditions that are (presumably) responsible for a landslide occurrence were determined. This basically allowed propagating the rainfall measurement uncertainty as opposed to the uncertainty estimations proposed in the literature, mainly obtained using resampling approaches (i.e.

Peruccacci et al., 2012) useful to determine a more reliable rainfall threshold (**Fig. 5**).

Inspection of **Figs. 3 and 5** shows that rainfall conditions reconstructed using the expert method and the automated procedure have a similar general trend, and that in general, the largest differences occur for the events with the lowest cumulated rainfall. The total number of events derived by the automated procedure (114 points in **Fig. 5A** and 89 points in **Fig. 5B**) is lower than that obtained by the expert method (182 points in **Fig. 3A** and 124 points in **Fig. 3B**) and that the decrease is larger for short durations (D < 24 h). This is explained since those events characterized by a large uncertainty, according to **Eqs. (1)** and **(2)**, are discarded from rainfall threshold analysis.

To define thresholds from rainfall datasets obtained by the automated procedure (**Fig. 5)**, we used three different statistical, objective and automated methods: LS, QR and NLS described in Sections **5.1**, **5.2** and **5.3**. The LS is comparable with that proposed by Peruccacci et al. (2012); unlike in the mentioned method, the estimation of the uncertainty associated with the real rainfall conditions necessary to trigger each landslide was here considered. As in the expert method proposed by Peruccacci et al. (2012), rainfall threshold with a non-exceedance probability level of 5% determined by the LS method is the curve parallel to the best-fit line (corresponding to 50th percentile) and to the curves of any non-exceedance probability levels. In the expert method, uncertainty decreases by increasing the number of data analysed (Peruccacci et al., 2012). In the automated procedure, uncertainty decreases when the uncertainty of the rainfall events associated with landslides reduces. The two thresholds defined using the LS method have a relatively small uncertainty; they represent well the general trend of the data, but they are not able to represent the lower bound of the empirical (D,E) data points for all durations (**Fig. 7A,B**).

Comparison of the results for the LS method in **Table 1** with those in **Table 2** shows that the slope of the power law thresholds (γ) obtained with the expert method are lower than those with the automated procedure.

Visual inspection of **Fig. 7C,D** derived using the QR method reveals that the power law threshold in the log-log coordinates (**Eq. 4)** performed well to bound the data distribution for duration $D >$ 24 h but is less appropriate for shorter durations events ($D <$ 24 h) where the threshold underestimates the rainfall. This is a consequence of the reduced number of empirical data points with short rainfall duration ($D <$ 24 h), but also a result of the fact that the lower bound of the cloud of the empirical data points with $D <$ 24 h is almost horizontal, and does not follow the increasing trend prescribed by **Eq. (4).** The thresholds obtained adopting the NLS model, based on **Eq. (5)** with three parameters (**Fig. 7E,F)** works properly as lower boundaries of the empirical data points for the entire range of rainfall duration. In particular, we observed that for $D <$ 24 h, a stretch of the curve is horizontal and therefore E values are independent of duration. For $D >$ 24 h the NLS thresholds are similar to the QR thresholds. For very long rainfall durations ($D >$ 200 h), the NLS thresholds are slightly higher than the LS and QR thresholds (**Fig. 6A,C**). The better performance of the NLS thresholds is obtained at expense of a significantly larger uncertainly, but only for $D <$ 24 h. We feel that, despite the larger uncertainty for the short duration event, the two thresholds minimized the problem of the underestimation of rainfall required to trigger landslides in Umbria.

Table 2 shows the results of the rainfall threshold analysis by the automated procedure, using a period of 72 h without rain to separate two rainfall events. **Figs. 7 and 8** show thresholds obtained with the statistical methods previously described. In this case, thresholds obtained with rain gauge and satellite data of **Table 2** also reveal that the values of α for satellite rainfall threshold are lower than those obtained for rain gauge rainfall threshold, while the values of γ are very similar. Moreover, the significance levels reported in the table show that adding a third parameter to the power-law threshold model (i.e. as for the NLS method) is significant and do not imply over-parameterization problems.

We also verified that the thresholds obtained with the three statistical methods cited above, using different periods without rain to separate two rainfall events (24, 48, and 96 h), are statistically undistinguishable, and the uncertainty associated with thresholds overlap. The observed differences are mostly in the length of the events. For longer separation periods, the duration of the events increases, and the range of duration for the validity of the thresholds also increases. This is more evident for rainfall events associated with regional frontal systems characterized by prolonged, low-intensity rainfall. Convective events, typical of the summer period and characterized by short duration and high rainfall rates, are less sensible to the length of the separation period.

In addition, a systematic application of the QR method for non-exceedance probability levels from 5% to 95% was carried out, using a period of 72 h without rain to separate two rainfall events. Results reveal that the thresholds obtained for the different quantiles, have different slopes (γ values) (**Fig. 10A**). This suggests that, shifting the threshold parallel to that obtained for the 50th percentile to obtain other thresholds for different non-exceedance probabilities values (e.g. 5%) is not always representative. Moreover, the uncertainty also varies with the different non-exceedance probabilities levels: the uncertainty for the 50th percentile is smaller than those for lower percentile values (**Fig. 10B**). Therefore, defining a lower threshold (e.g., the 5%

threshold) shifting that obtained for the 50th percentile together with its uncertainty is inappropriate in this case.

Significant results were obtained when validating the thresholds defined with different statistical approaches using satellite and rain gauge data. The analysis of **Fig. 9** supported by numerical results in **Table 3**, reveals good performances of the thresholds to forecast the possible landslide occurrence for independent rainfall conditions (i.e. not used in the threshold definition) derived from the UFC dataset. Indeed, the percentages of rainfall conditions triggering landslides below the thresholds reported in Table 3 are close to the 5% non-exceedance probability used to define the thresholds (i.e. the probability level expected when applying the threshold with new landslide data).

Despite the good validation results, the three approaches do not perform similarly (i.e. do not have the same effectiveness) when applied to derive rainfall thresholds for the possible landslide occurrence using new and independent landslide information. Indeed, comparison of **Tables 2 and 4** reveals that only NLS produces comparable threshold parameters (i.e. within the expected lower and upper parameter uncertainty boundaries), when applied to an independent landslide dataset. As a result, NLS is the most effective methods to derive rainfall thresholds and should be preferred among the others, particularly when using landslide dataset with a limited knowledge on the criteria used for the landslide inventory collection, and on the spatial and temporal accuracy of the collected information.

7. Conclusions

We proposed an automated procedure to reconstruct the *ED* rainfall conditions that have induced landslides using rain gauge and satellite data for the Umbria region, central Italy. The rainfall events derived by the procedure are reproducible and objective and include the uncertainties of the (D,E) rainfall data, unlike those obtained by the expert method.

Among the various statistical methods used for defining thresholds from rainfall data derived by the automated procedure, the NLS method performed better in identifying the boundary conditions on the entire range of rainfall durations. The better performance of the NLS thresholds is obtained at the expense of a larger uncertainty for the shorter duration ($D < 24$ h). We think that, despite the large uncertainty for the short duration events, the two thresholds minimized the problem of the underestimation of the rainfall required to trigger landslides in the Umbria region. The thresholds obtained by the QR method perform well for longer rainfall durations ($D > 24$ h), providing results similar to the NLS method, but are less appropriate for shorter duration values ($D < 24$ h). On the contrary, LS method does not represent properly the lower bound of empirical data points for all durations. These results show that the LS method is inappropriate for the estimation of rainfall thresholds in the Umbria region. These thresholds, if used in a landslide warning system, would underestimate the rainfall conditions responsible for landslide occurrence, resulting in a significant number of potential false alarms. In addition, despite the similar validation performances of the three statistical methods, NLS should also be preferred given its higher effectiveness when defining thresholds using a landslide dataset with a limited knowledge on the criteria used for the landslide inventory collection and on the spatial and temporal accuracy of the collected information.

The comparison of the parameters of rainfall thresholds, obtained with rain gauge and satellite data and using different statistical methods, reveals that the thresholds obtained from satellite estimates are lower than those obtained from rain gauge measurements. This agrees with the underestimation of the "ground" rainfall data observed by Rossi et al. (submitted) and reference therein, by comparing rain gauge measurements and satellite rainfall estimates. Finally, the proposed method can be applied using different rainfall data estimates, such as radar estimated precipitation, or new GPM satellite rainfall products to derive rainfall thresholds for the possible landslide occurrence.

Acknowledgments

This research was supported by the Italian National Civil Protection Department (DPC). SL was supported by a grant of DPC. We are grateful to the NASA TMPA for providing the TRMM product version 6 (V6) 3B42, to the DPC for the rainfall data in Umbria, to the UFC for a landslide dataset, and to the Umbria fire brigades for valuable information on landslide events.

References

Aleotti, P.: A warning system for rainfall-induced shallow failures. Eng Geol, 73, 247-265, 2004.

Aleotti, P., and Chowdhury, R.: Landslide hazard assessment: Summary review and new perspectives, Bull. Eng. Geol. Environ., 58, 21-44, 1999. doi:10.1007/s100640050066.

Antonini, G., Ardizzone, F., Cardinali, M., Galli, M., Guzzetti, F. and Reichenbach, P.: Surface deposits and landslide inventory map of the area affected by the 1997 Umbria-Marche earthquakes, Boll. Soc. Geol. It., 121(1), 843–853, 2002.

Bates, D. M., and Watts, D.G.: Nonlinear Regression Analysis and Its Applications. Wiley Book, New York, 1988, ISBN: 0471-816434.

Berti, M., Martina, M.L.V., Franceschini, S., Pignone, S., Simoni, A., and Pizziolo, M.: Probabilistic rainfall thresholds for landslide occurrence using a Bayesian approach, J. Geoph. Res., 117, F04006, 2012, doi:10.1029/2012JF002367.

Biafore, M., Braca, G., De Blasio, A., Martone, M., Onorati, G., and Tranfaglia, G.: Il monitoraggio ambientale dei territori campani a rischio di frane e di alluvioni: lo sviluppo della rete idropluviometrica del Servizio Idrografico e Mareografico Nazionale. Unpublished report, 2001.

Bolley, S. and Oliaro, P.: Analisi dei debris flows in alcuni bacini campione dell'Alta Val Susa. Geoingegneria Ambientale e Mineraria (GEAM), March, 69–74, 1999.

Brunetti, M.T., Peruccacci, S., Rossi, M., Luciani, S., Valigi, D., and Guzzetti, F.: Rainfall thresholds for the possible occurrence of landslides in Italy. Nat. Hazard Earth Sys., 10, 447–458, 2010.

Caine, N.: The rainfall intensity-duration control of shallow landslides and debris flows. Geogr. Ann. A., 62, 23–27, 1980.

Calcaterra, D., Parise, M., Palma, B., and Pelella, L.: The influence of meteoric events in triggering shallow landslides in pyroclastic deposits of Campania, Italy. In: Proceedings

8th International Symposium on Landslides, edited by: Bromhead, E., Dixon, N., and Ibsen, M. L., A. A. Balkema, Cardiff, 1, 209–214, 2000.

Cannon, S.H., and Ellen, S.D.: Rainfall conditions for abundant debris avalanches, San Francisco Bay region, California. Calif. Geol., 38, 267–272, 1985.

Cardinali, M., Ardizzone, F., Galli, M., Guzzetti, F. and Reichenbach, P.: Landslides triggered by rapid snow melting: the December 1996-January 1997 event in Central Italy, pp. 439–448, 2000.

Cardinali, M., Galli, M., Guzzetti, F., Ardizzone, F., Reichenbach, P. and Bartoccini, P.: Rainfall induced landslides in December 2004 in south-western Umbria, central Italy: types, extent, damage and risk assessment, NHESS, 6, 237–260, 2006.

Ceriani, M., Lauzi, S., and Padovan, N.: Rainfall and landslides in the Alpine area of Lombardia Region, central Alps, Italy. In: Interpraevent Int Symposium, Bern, 2, 9–20, 1992.

Cevasco, A., Sacchini, A., Robbiano, A., and Vincenzi, E.: Evaluation of rainfall thresholds for triggering shallow landslides on the Genoa municipality area (Italy): the case study of the Bisagno Valley. Italian Journal of Engineering Geology and Environment, 1, 35–50, 2010.

Chambers, J.M.: Linear models. In: Statistical Models, edited by: S, Chambers, J.M., and Hastie, T.J., Wadsworth and Brooks/Cole, Pacific Grove, California, 1992.

Crosta, G.B., and Frattini, P.: Rainfall thresholds for triggering soil slips and debris flow. In: Proceedings 2nd EGS Plinius Conference on Mediterranean Storms, edited by: Mugnai, A., Guzzetti, F., and Roth, G., Siena, publication no 2547, 463-487, 2001.

Cruden, D.M., and Varnes, D.J.: Landslide types and processes. In: Landslides, Investigation and Mitigation, Transportation Research Board, edited by: Turner, A. K., and Schuster, R. L., Special Report 247, Washington, DC, 36-75, 1996.

Dahal, R.K., and Hasegawa, S.: Representative rainfall thresholds for landslides in the Nepal Himalaya. Geomorphology 100, 429-443, 2008.

Deganutti, A.M., Marchi, M., and Arattano, M.: Rainfall and debris flow occurrence in the Moscardo basin (Italian Alps). In: Wieczorek, G.F., Naeser, N.D. (Eds.), Proceedings 2nd International Conference on Debris-Flow Hazards Mitigation: Mechanics, Prediction, and Assessment. American Society of Civil Engineers, Taipei, Taiwan, 67-72, 2000.

Efron, B.: Bootstrap methods: another look at the jackknife. Ann. Stat., 7, 1-26, 1979.

Efron, B. and Tibshirani, R.J.,: An introduction to the bootstrap. Chapman and Hall, New York, 1994.

Esposito, E., Porfido, S., Simone, S., Mastrolorenzo, G. and Iaccarino, G.: Landslides and other surface effects induced by the 1997 Umbria-Marche seismic sequence, Eng. Geol., 58(3-4), 353–376, 2000.

Floris, M., and Bozzano, F.: Evaluation of landslide reactivation: a modified rainfall threshold model based on historical records of rainfall and landslides. Geomorphology, 94, 40–57, 2008.

Frattini, P., Crosta, G., and Sosio, R.: Approaches for defining thresholds and return periods for rainfall-triggered shallow landslides. Hydrol. Process. 23, 1444–1460, 2009.

Gariano, S.L., Brunetti M.T., Iovine G., Melillo M., Peruccacci S., Terranova O., Vennari C., Guzzetti F.: Calibration and validation of rainfall thresholds for shallow landslide forecasting in Sicily, southern Italy. Geomorphology, 228, 653–665, 2014, doi:10.1016/j.geomorph.2014.10.019.

Giannecchini, R.: Rainfall triggering soil slips in the southern Apuan Alps (Tuscany, Italy), ADGEO, 2, 21–24, 2005.

Giannecchini, R., Galanti, Y., and Avanzi, G.D.: Critical rainfall thresholds for triggering shallow landslides in the Serchio River Valley (Tuscany, Italy). Nat Haz Earth Sys Sci, 12(3), 829–842, 2012, doi:10.5194/nhess-12-829-2012.

Godt, J.W., Baum, R.L., and Chleborad, A.F.: Rainfall characteristics for shallow landsliding in Seattle, Washington, USA. Earth Surf Process Landforms 31, 97–110, 2006.

Guadagno, F.M.: Debris flows in the Campanian volcaniclastic soil (Southern Italy). In: Proceedings International Conference on slope stability, Isle of Wight: edited by: Telford, T., 125–130, 1991.

Guzzetti, F., Cardinali, M., and Reichenbach, P.: The influence of structural setting and lithology on landslide type and pattern. Environ Eng Geosci, 2, 531–555, 1996.

Guzzetti, F., Reichenbach, P., Cardinali, M., Ardizzone, F. and Galli, M.: The impact of landslides in the Umbria region, central Italy, NHESS, 3, 469–486, 2003.

Guzzetti, F., Peruccacci, S., Rossi, M., and Stark, C.P.: Rainfall thresholds for the initiation of landslides in central and southern Europe. Meteorol. Atmos. Phys., 98, 239–267, 2007.

Guzzetti, F., Peruccacci, S., Rossi, M., and Stark, C.P.: The rainfall intensity-duration control of shallow landslides and debris flow: an update. Landslides, 5(1), 3–17, 2008.

Huffman, G. J., Bolvin, D. T., Braithwaite, D., Hsu, K., Joyce, R., Xie, P., & Yoo, S. H.: NASA Global Precipitation Measurement (GPM) Integrated Multi-satellitE Retrievals for GPM (IMERG). Algorithm Theoretical Basis Document, Version 4.1, NASA, 25, 2013.

Huffman, G.J., Adler, R.F., Bolvin, D.T., Gu, G., Nelkin, E.J., Bowman K.P., et al.: The TRMM Multisatellite Precipitation Analysis (TMPA): quasi-global, multiyear, combined-sensor precipitation estimates at fine scales. J. Hydrometeorol., 8, 38–55, 2007, doi:10.1175/JHM560.1.

Huffman, G.J., Adler, R.F., Bolvin, D.T., and Nelkin, E.J.: The TRMM Multi-satellite Precipitation Analysis (TMPA). In: Satellite Applications for Surface Hydrology, chapter 1, edited by: Hossain, F., and Gebremichael, M., Springer Verlag, 2010, ISBN: 978-90-481-2914-0, 3–22, 2010, available at ftp://meso.gsfc.nasa.gov/agnes/huffman/papers/TMPA_hydro_rev.pdf

Innes, J.L.: Debris flows. Prog. Phys. Geog., 7, 469–501, 1983.

Jaiswal, P., and van Westen, C.J.: Rainfall-based temporal probability for landslide initiation along transportation routes in Southern India. Landslide Processes: From Geomorphologic Mapping to Dynamic Modeling. France, pp 139–143, 2009.

Kirschbaum, D.B., Adler, R., Hong, Y., Kumar, S., Peters-Lidard, C., and Lerner-Lam, A.: Advances in landslide nowcasting: evaluation of a global and regional modeling approach. Environ. Earth Sci., 6, 1683–1696, 2012.

Koenker, R. and Bassett, G.: Regression quantiles. Econometrica, 46, 33–50, 1978.

Lagomarsino, D., Segoni, S., Fanti, R., and Catani, F.:Updating and tuning a regional-scale landslide early warning system. Landslides 10, 91–97, 2013 doi: 10.1007/s10346-012-0376-y

Lazzari, M., Piccarreta, M., and Capolongo, D.: Landslide Triggering and Local Rainfall Thresholds in Bradanic Foredeep, Basilicata Region (Southern Italy). In: Margottini, C., Canuti, P. and Sassa, K. (eds.), Landslide Science and Practice, 2, 671–677, 2013, doi: 10.1007/978-3-642-31445-2_88, Springer-Verlag Berlin Heidelberg.

Li, C., Ma, T., Zhu, X., and Li, W.:The power–law relationship between landslide occurrence and rainfall level. Geomorphology 130, 221–229, 2011. Marchi, L., Arattano, M., and Deganutti, A.M.: Ten years of debris-flow monitoring in the Moscardo Torrent (Italian Alps). Geomorphology, 46, 1–17, 2002.

Marra, F., Nikolopoulos, E.I., Creutin, J.D., and Borga, M., 2014. Radar rainfall estimation for the identification of debris-flow occurrence thresholds. J. Hydrol. (conditionally accepted).

Martelloni, G., Segoni, S., Fanti, R., and Catani, F.: Rainfall thresholds for the forecasting of landslide occurrence at regional scale. Landslides, 9, 485–495, 2012, doi:10.1007/s10346-011-0308-2.

Melillo, M., Brunetti, M.T., Peruccacci, S., Gariano, S.L. and Guzzetti, F.: An algorithm for the objective reconstruction of rainfall events responsible for landslides. Landslides, 2014. doi:10.1007/s10346-014-0471-3, Springer-Verlag Berlin Heidelberg, 2014

Morrissey, M.L., Maliekal, J.A., Greene, J.S.,and Wang, J.: The uncertainty of simple spatial averages using rain gauge networks. Water Resour. Res. 31, 2011–2017,1995.

Nikolopoulos, E.I., Crema, S., Marchi, L., Marra, F., Guzzetti, F. and Borga, M.: Impact of incertainty in rainfall estimation on the identification of rainfall thresholds for debris flow occurrence. Geomorphology, 221, 286-297, 2014.

Penna, D., Tromp-Van Meerveld, H.J., Gobbi, A., Borga, M., and Dalla Fontana, G.: The influence of soil moisture on threshold runoff generation processes in an alpine headwater catchment. Hydrol. Earth Syst. Sci. 15, 689–702, 2011.

Peruccacci, S., Brunetti, M.T., Luciani, S., Vennari, C., and Guzzetti, F.: Lithological and seasonal control on rainfall thresholds for the possible initiation of landslides in central Italy. Geomorphology, 139–140, 79-90, 2012, doi:10.1016/j.geomorph.2011.10.005.

R Core Team: R: A language and environment for statistical computing. R Foundation for Statistical Computing, Vienna, Austria, 2015, URL http://www.R-project.org/

Rosi, A., Segoni, S., Catani, F., and Casagli, N.: Statistical and environmental analyses for the definition of a regional rainfall threshold system for landslide triggering in Tuscany (Italy). J Geogr Sci, 22(4), 617–629, 2012, doi:10.1007/s11442-012-0951-0.

Rossi, M., Kirschbaum, D., Luciani, S., Mondini, A.C., and Guzzetti, F. Comparison of satellite rainfall estimates and rain gauge data in Italy: impact on the hydrogeological modelling. (submitted to Remote Sensing of Environment)

Rossi, M., Kirschbaum, D., Luciani, S., Mondini, A.C., and Guzzetti, F.: TRMM satellite rainfall estimates for landslide early warning in Italy: preliminary results. Proceeding SPIE 8523, Remote Sensing of the Atmosphere, Clouds, and Precipitation IV, 85230D (8 November 2012), 2012, doi:10.1117/12.979672.

Rossi, M., Peruccacci, S., Brunetti, M. T., Marchesini, I., Luciani, S., Ardizzone, F., Balducci, V., Bianchi, C., Cardinali, M., Fiorucci, F., Mondini, A. C., Reichenbach, P., Salvati, P., Santangelo, M., Bartolini, D., Gariano, S. L., Palladino, M., Viero, A., Vessia, G., Antronico, L., Borselli, L., Deganutti, A. M., Iovine, G. G. R., Luino, F., Parise, M., Polemio, M. and Guzzetti, F.: SANF: National warning system for rainfall-induced landslides in Italy, In: Landslides and Engineered Slopes: Protecting Society through Improved Understanding – Eberhardt et al. (eds) Taylor & Francis Group, London, ISBN 978-0-415-62123-6, 2, 1895–1899, 2012b.

Rossi M., Mondini A. C., Luciani S., Kirschbaum D., Valigi D., and Guzzetti F. Probabilistic Prediction of Landslides Induced by Rainfall. In Vulnerability, uncertainty, and risk quantification, mitigation, and management. Proceedings of the second International Conference On Vulnerability And Risk Analysis And Management (ICVRAM) and the sixth International Symposium On Uncertainty Modeling And Analysis (ISUMA). 2014.

Rossi M., Mondini A.C., Luciani S., Kirschbaum D., Valigi D., and Guzzetti F. A new probabilistic clustering approach for predicting rainfall induced landslides. First International Workshop on Warning Criteria for Active Slides (IWWCAS). Courmayeur, Italia, 10/12 June 2013. 2013.

Saito, H., Nakayama, D., and Matsuyama, H.: Relationship between the initiation of a shallow landslide and rainfall intensity-duration thresholds in Japan. Geomorphology, 118, 167–175, 2010.

Salvati, P., Bianchi, C., Rossi, M. and Guzzetti, F. Societal Landslide and Flood Risk in Italy. Nat. Haz. Earth Sys. Sci., 10, 465–83, 2010.

Salvati, P., Marchesini, I., Balducci, V., Bianchi, C. and Guzzetti, F. A New Digital Catalogue of Harmful Landslides and Floods in Italy. In: Margottini, C., Canuti, P. and Sassa, K. (eds.),Landslide Science and Practice, 3, 409–414, Springer-Verlag Berlin Heidelberg, doi:10.1007/978-3-642-31310-3_56. 2013.

Segoni, S., Leoni, L., Benedetti, A. I., Catani, F., Righini, G., Falorni, G., Gabellani, S., Rudari, R., Silvestro, F. and Rebora, N.: Towards a definition of a real-time forecasting network for rainfall induced shallow landslides, NHESS, 9, 2119–2133, 2009.

Segoni, S. Rosi, A., Rossi, G., Catani, F., and Casagli, N.: Analysing the relationship between rainfalls and landslides to define a mosaic of triggering thresholds for regional scale warning systems Nat. Hazards Earth Syst. Sci. Discuss., 2, 2185-2213, 2014. www.nat-hazards-earth-syst-sci-discuss.net/2/2185/2014/doi:10.5194/nhessd-2-2185-2014

Shamsudin, S., Dan'azumi, S., and Aris, A.: Effect of storm separation time on rainfall characteristics - a case study of Johor, Malaysia. Eur. J. Sci. Res. 45(2),162-167, 2010.

Staley, D., Kean, J., Cannon, S., Schmidt, K., Laber, J.: Objective definition of rainfall intensity–duration thresholds for the initiation of post-fire debris flows in southern California. Landslides, 10, 547–562, 2013.

Tiranti, D., and Rabuffetti, D.: Estimation of rainfall thresholds triggering shallow landslides for an operational warning system implementation. Landslides, 7, 471–481, 2010, doi: 10.1007/s10346-010-0198-8.

Tabios, G.Q., and Salas, J.D.: A comparative analysis of techniques for spatial interpolation of precipitation. JAWRA J. Am. Water Resour. Assoc. 21, 365–380, 1985.

Torri, D., Borselli, L., Guzzetti, F., Calzolari, M. C., Bazzoffi, P., Ungaro, F., Bartolini, D., Salvador Sanchis M. P. Italy In: Boardman, J. and Poesen, J. (eds.), Soil Erosion in Europe, 1.20, 245–261, John Wiley & Sons, Ltd, ISBN: 0-470-85910-5, 2006.

Vennari, C., Gariano, S.L., Antronico, L., Brunetti, M.T., Iovine, G.G.R., Peruccacci, S., Terranova, O.G. and Guzzetti, F. Rainfall Thresholds for Shallow Landslide Occurrence in Calabria, Southern Italy. Nat. Haz. Earth Sys. Sci., 14(2), 317–30, 2014, doi:10.5194/nhess-14-317-2014.

Verworn, A., and Haberlandt, U.: Spatial interpolation of hourly rainfall - effect of additional information, variogram inference and storm properties. Hydrol. Earth Syst. Sci. 15, 569–584, 2011.

Vessia, G., Parise, M., Brunetti, M.T., Peruccacci, S., Rossi, M., Vennari, C., and Guzzetti, F.: Automated reconstruction of rainfall events responsible for shallow landslides. Nat. Hazards Earth Syst. Sci. Discuss., 2, 2869–2890, 2014. doi:10.5194/nhessd-2-2869-2014

Wilkinson, G.N., and Rogers, C.E.: Symbolic descriptions of factorial models for analysis of variance. Appl. Stat.-J. Roy. St. C., 22(3), 392–399, 1973.

TABLES

Table 1. *ED* rainfall threshold parameters (α and γ) estimated for the Umbria region for a non-exceedance probability of 5% using rain gauge measurements and TRMM satellite rainfall estimates, and the value of the uncertainty associated to the thresholds. α_{inf} and γ_{inf} are lower boundaries and α_{sup} and γ_{sup} are upper boundaries of uncertainty. Thresholds defined using the method proposed by Peruccacci et al. (2012) based on rainfall conditions reconstructed with the expert method.

Rainfall data	α_{inf}	α	α_{sup}	γ_{inf}	γ	γ_{sup}
Rain gauge	5.8	6.6	7.4	0.39	0.41	0.43
Satellite	2.1	2.4	2.7	0.36	0.39	0.42

Table 2. *ED* rainfall thresholds parameters (t, α and γ) estimated for the Umbria region for an non-exceedance probability of 5% using rain gauge measurements and TRMM satellite rainfall estimates. t_{inf}, α_{inf} and γ_{inf} are lower boundaries and t_{sup}, α_{sup} and γ_{sup} are upper boundaries for the model parameters estimated exploiting the Least Square (LS), the Quantile Regression (QR), and the Nonlinear Least Square (NLS) methods. All data processing was run using a period of 72 h without rain to separate two rainfall events. Significance of threshold parameters, estimated from *t*-test statistics and corresponding (two-sided) *p*-values, are reported in the table and codified following the schema at the bottom.

RAIN GAUGES									
Method	t_{inf}	t	t_{sup}	α_{inf}	α	α_{sup}	γ_{inf}	γ	γ_{sup}
LS	-	-	-	4.90	5.20*****	5.60	0.56	0.56*****	0.57
QR	-	-	-	0.25	0.43*****	0.74	0.82	0.88*****	0.93

NLS	2.3	9.8****	15.0	0.09	0.01***	0.01	1.15	1.53*****	1.56
SATELLITE									
Method	t_{inf}	t	t_{sup}	α_{inf}	α	α_{sup}	γ_{inf}	γ	γ_{sup}
LS	-	-	-	4.40	4.60*****	4.70	0.31	0.31*****	0.33
QR	-	-	-	0.35	0.47*****	0.48	0.54	0.6*****	0.64
NLS	1.1	2.6***	4.1	0.01	0.03***	0.12	0.85	1.2*****	1.39

Significance codes and associated p-value ranges: '*****' [0, 0.001] '****']0.001, 0.01] '***']0.01, 0.05] '**']0.1, 1] '*']0.05, 0.1]

Table 3. Comparison of the number and percentage of new rainfall conditions triggering landslide (not used in the threshold identification) below the thresholds, estimated using different methods for rain gauge and satellite rainfall data. The rainfall conditions were derived starting from the independent landslide dataset provided by the Umbria Functional Centre (UFC) of the Italian Civil Protection Department.

Threshold method	Events below rain gauge threshold # (%)	Events below satellite threshold # (%)
LS	7 (3.7)	23 (12.0)
QR	9 (4.7)	9 (4.7)
NLS	11 (5.7)	23 (12.0)

Table 4. *ED* rainfall thresholds parameters (t, α and γ) estimated for the Umbria region for a non-exceedance probability of 5% using rain gauge measurements and satellite rainfall estimates starting from the landslides independent dataset provided by the Umbria Functional Centre of the Civil Protection Department, exploiting the Least Square (LS), the Quantile Regression (QR), and the Nonlinear Least Square (NLS) methods. All data processing was run using a period of 72 h without rain to separate two rainfall events.

RAIN GAUGES			
Method	t	α	γ
LS	-	0.10	0.88
QR	-	0.03	1.32
NLS	2.5	0.01	1.50
SATELLITE			
Method	t	α	γ
LS	-	0.10	0.64
QR	-	0.23	0.68
NLS	1.1	0.05	1.06

FIGURE CAPTIONS

Fig. 1. Map of the study area, the Umbria region, central Italy. Shades of colour portray elevation computed from a 90m DEM obtained by the NASA Shuttle Radar Topography Mission in February 2000. Small map of the study area shows simplified lithology: PO, post-orogenic sediments complex; FD, flysch deposits complex; CC, carbonate rocks complex; CH, chaotic deposits; VR, volcanic rocks complex. Pie chart summarizes the extent and percentage of the lithological complexes.

Fig. 2. Landslide and rainfall data for the Umbria Region. (A) Location of 187 rainfall-induced landslides (yellow dots) of the national catalogue modified in this study and of the 192 landslides of the UFC dataset collected in Umbria for the period 2002–2010. (B) Location of 60 rain gauges (red triangles) and 13 satellite centroids (blue dots). For both maps, shades of colour portray elevation computed from a 90m DEM obtained by the NASA Shuttle Radar Topography Mission in February 2000.

Fig. 3. Log-log plots showing rainfall duration D (x-axis) vs cumulated event rainfall E (y-axis) conditions that have resulted in landslides in Umbria in 2002–2010, reconstructed using the expert method. Red and green dots are rainfall conditions obtained using rain gauge measurements (A) and satellite rainfall estimates (B), respectively.

Fig. 4. Association schema between a landslide (yellow dot) and the representative rain gauges (R, red triangles) or satellite centroids (S, blue dots). Association, shown by solid lines for rain gauges and dotted lines for satellite centroids, depends on terrain elevation (h) and planimetric distance for rain gauges (d_R), and on planimetric distance for satellite centroids (d_S).

Fig. 5. Log-log plots show rainfall duration *D* (*x*-axis) vs cumulated event rainfall *E* (*y*-axis) conditions that have resulted in landslides in Umbria in 2002–2010 calculated exploiting the automated procedure. Red and green dots represent the (D_{50},E_{50}) median values of the rainfall conditions using rain gauge measurements (A) and satellite rainfall estimates (B), respectively. The horizontal and vertical lines show uncertainties associated with *D* and *E*, respectively.

Fig. 6. Least Square empirical rainfall threshold (obtained with the Frequentist method, F) corresponding to a 5% non-exceedance probability level defined using rain gauge measurements (A) and satellite rainfall estimates (B). The *ED* rainfall conditions (dots) were determined using the expert method. Shaded areas show uncertainty associated to the thresholds.

Fig. 7. Thresholds for possible landslide occurrence determined for a 5% non-exceedance probability level (coloured lines) starting from the rainfall conditions determined exploiting the automated procedure using rain gauge measurements (A, C, E) and satellite rainfall estimates (B, D, F). Orange lines (A, B) are thresholds defined using the LS method. Blue lines (C, D) are thresholds defined using the QR method. Violet curves (E, F) are thresholds defined using the NLS method. Shaded areas show uncertainties associated to the different threshold models.

Fig. 8. Comparison of the thresholds defined using the different methods (F, LS, QR, NLS) using rain gauge measurements (A) and satellite rainfall estimates (B). Shaded areas show uncertainty associated to the threshold models.

Fig. 9. Effectiveness of thresholds, derived for (A) rain gauge measurements and (B) satellite rainfall estimates (see Fig. 8), in forecasting rainfall conditions triggering landslide (red dots) reconstructed from the independent UFC dataset information.

Fig. 10. Thresholds defined using the QR method for different non-exceedance probability levels from 5% to 95%, exploiting *ED* rainfall conditions reconstructed from rain gauge data using a 72 h period for separating rainfall events (A). Uncertainty (shaded areas) associated to thresholds defined for the 5% and 50% non-exceedance probabilities levels (B).

Figure 1 (Color)

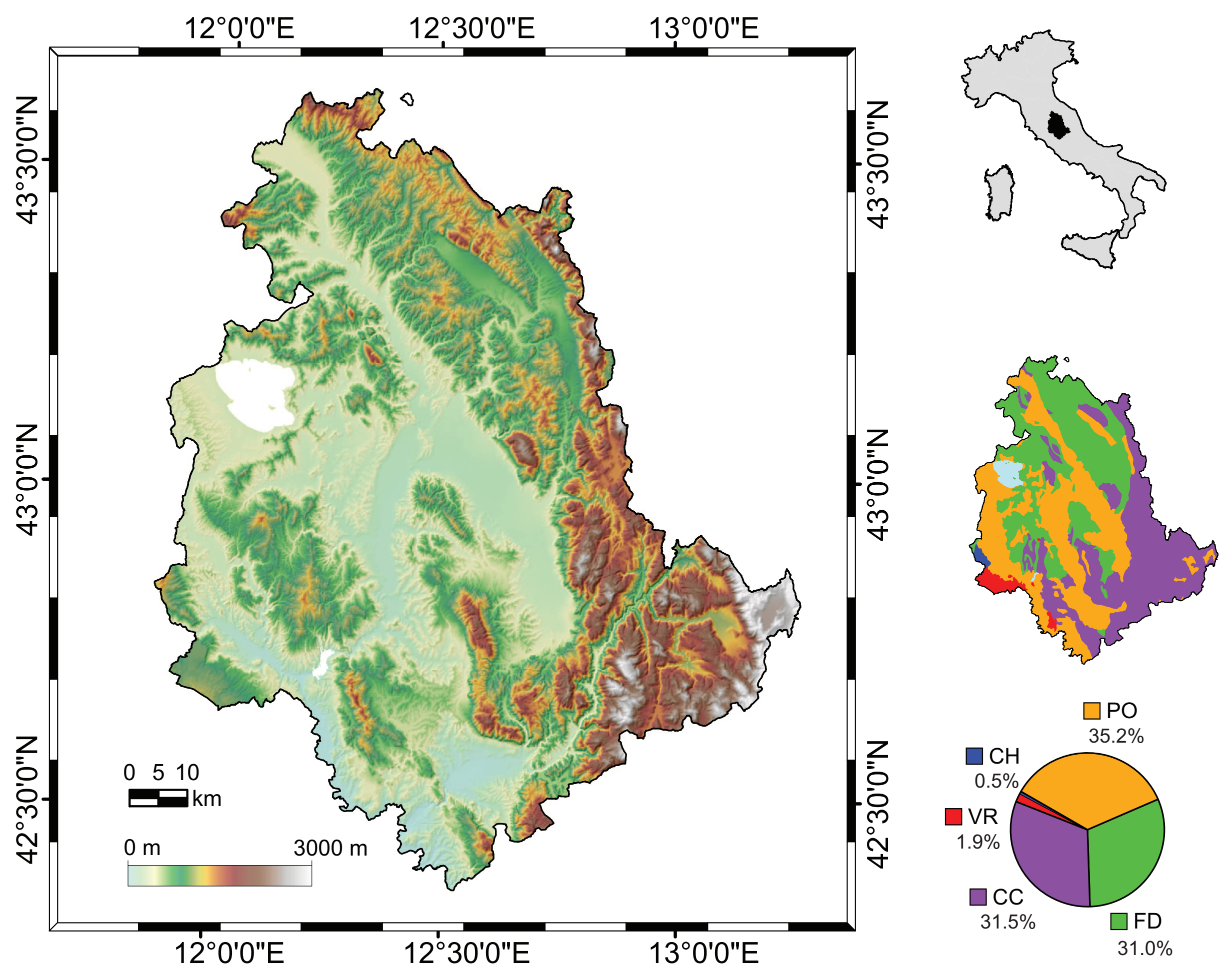

Figure 2 (Color)

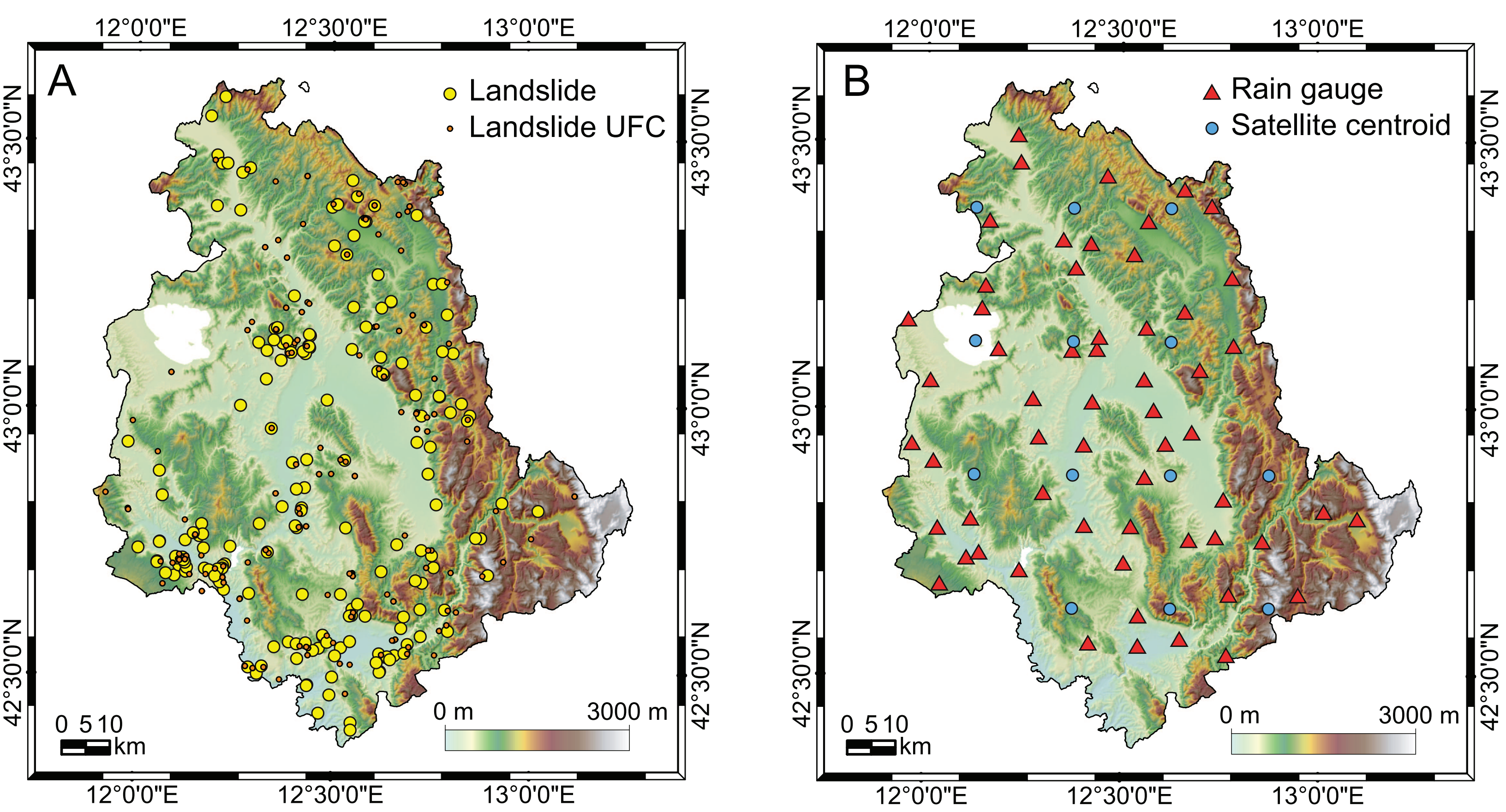

Figure 3 (Color)

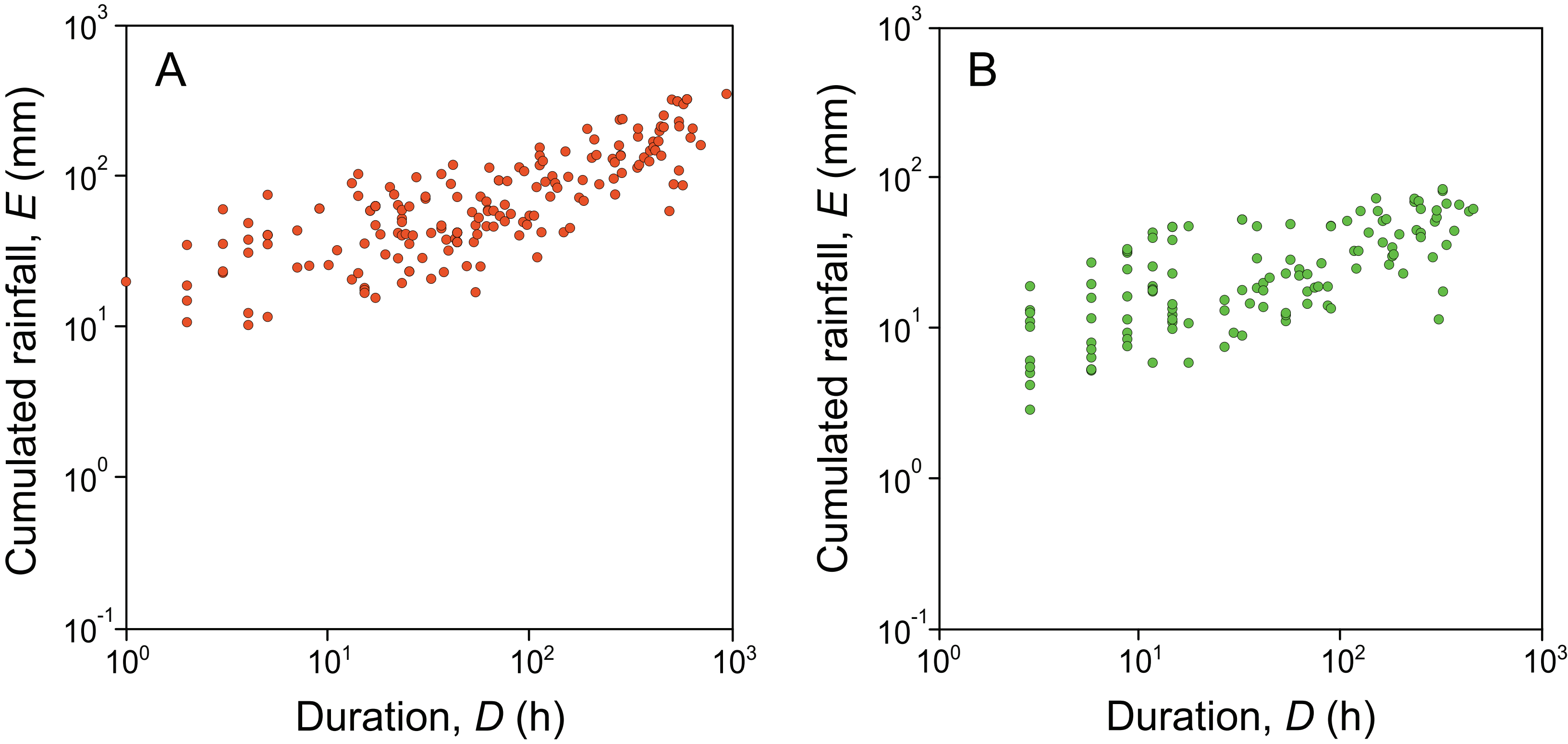

Figure 4 (Color)

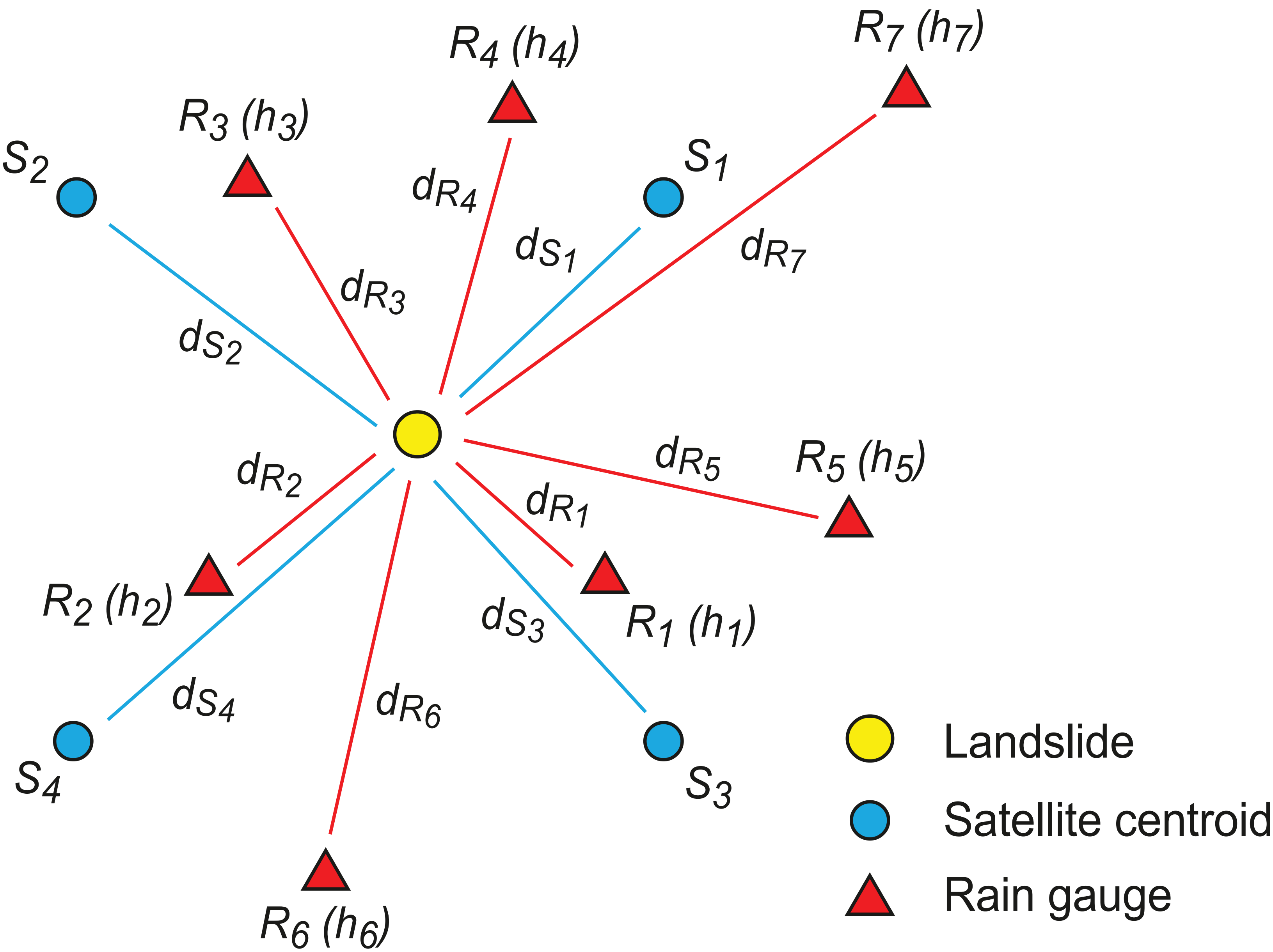

Figure 5 (Color)

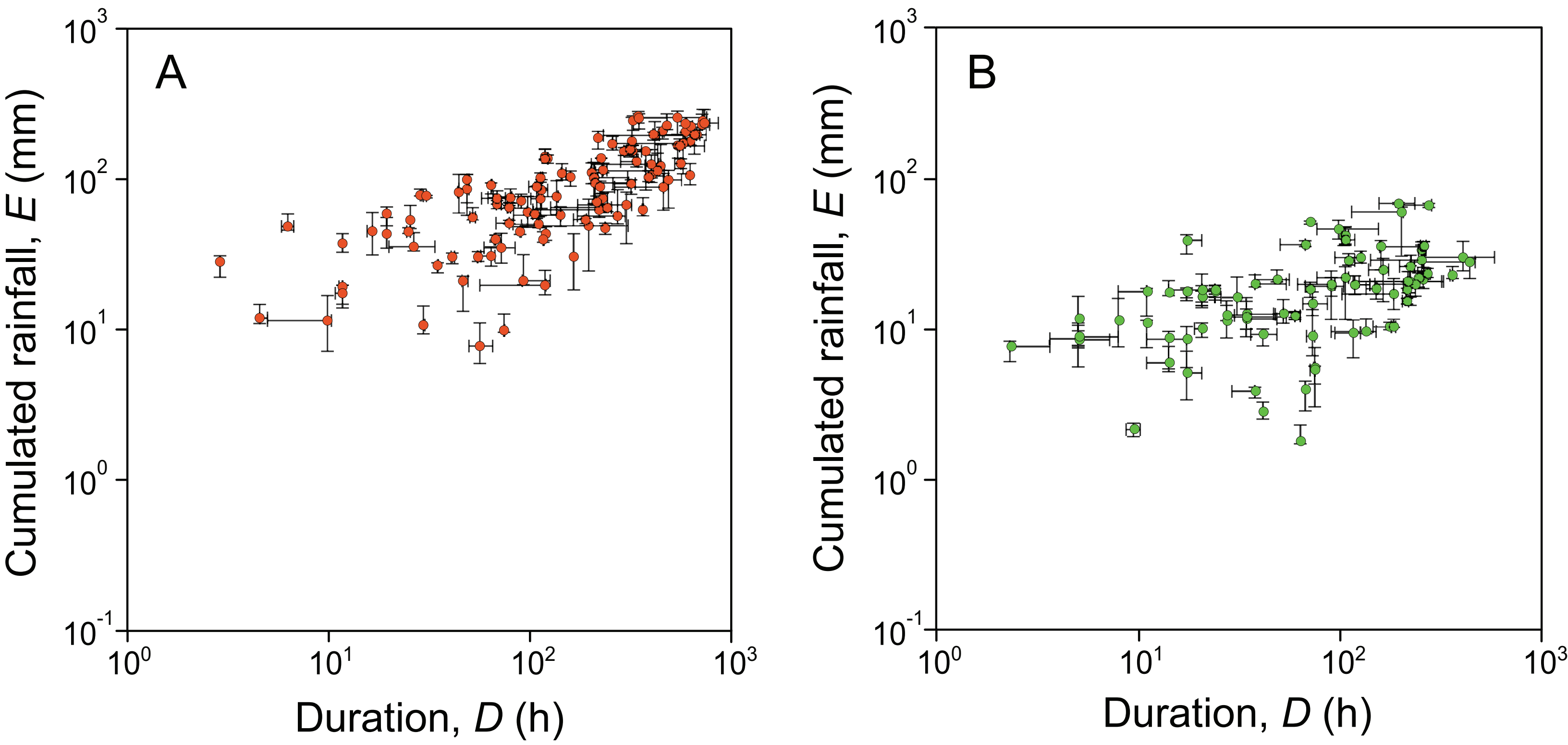

Figure 6 (Color)

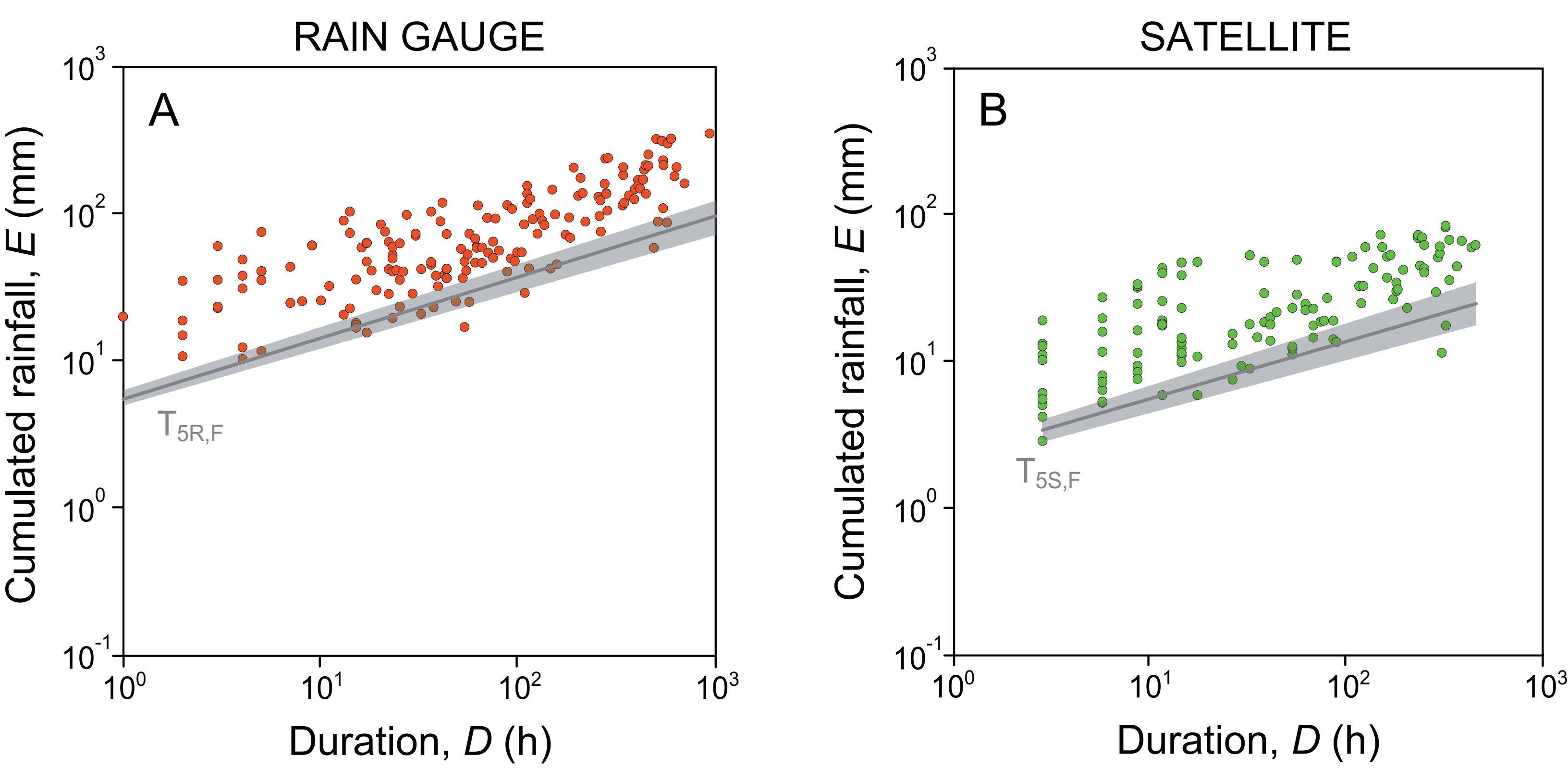

Figure 7 (Color)

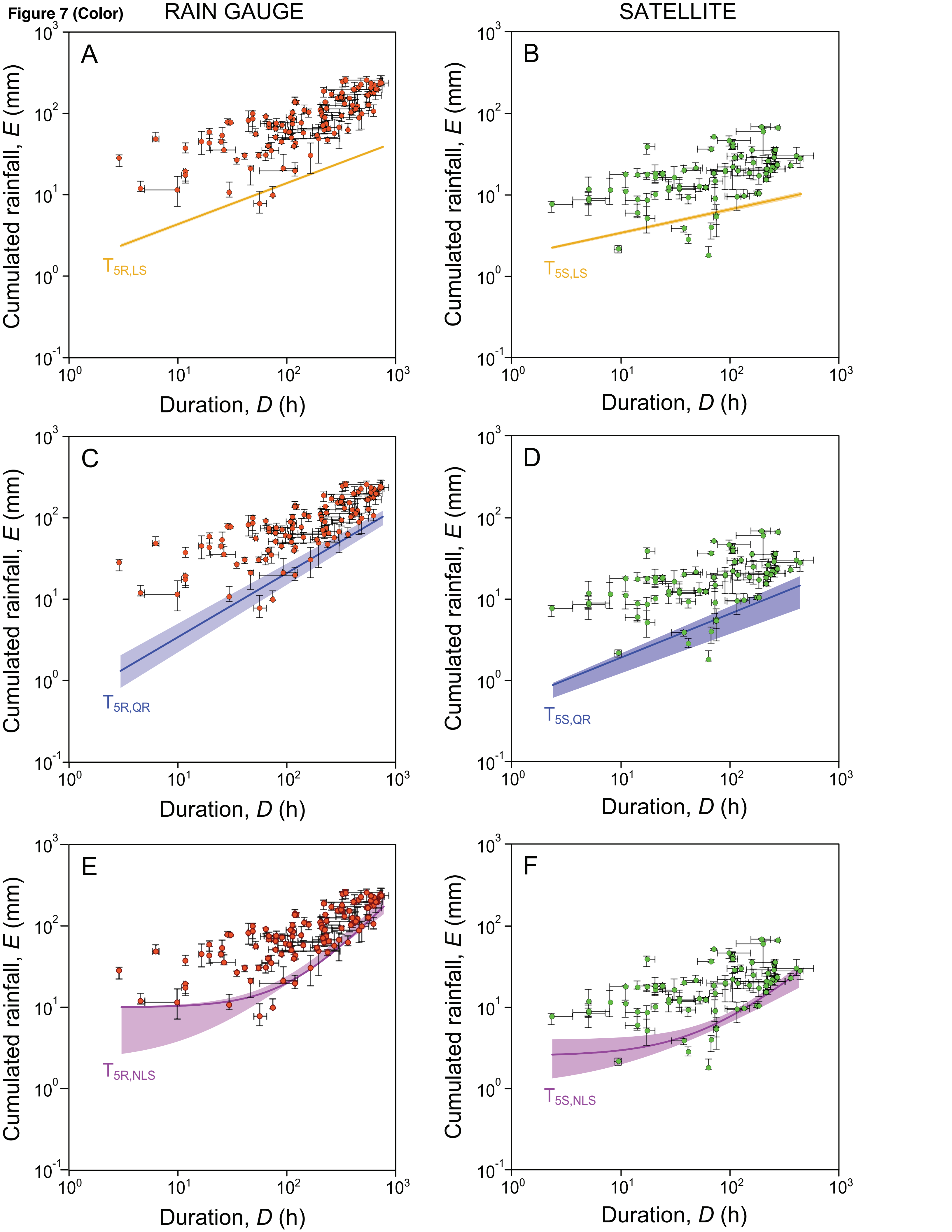

Figure 8 (Color)

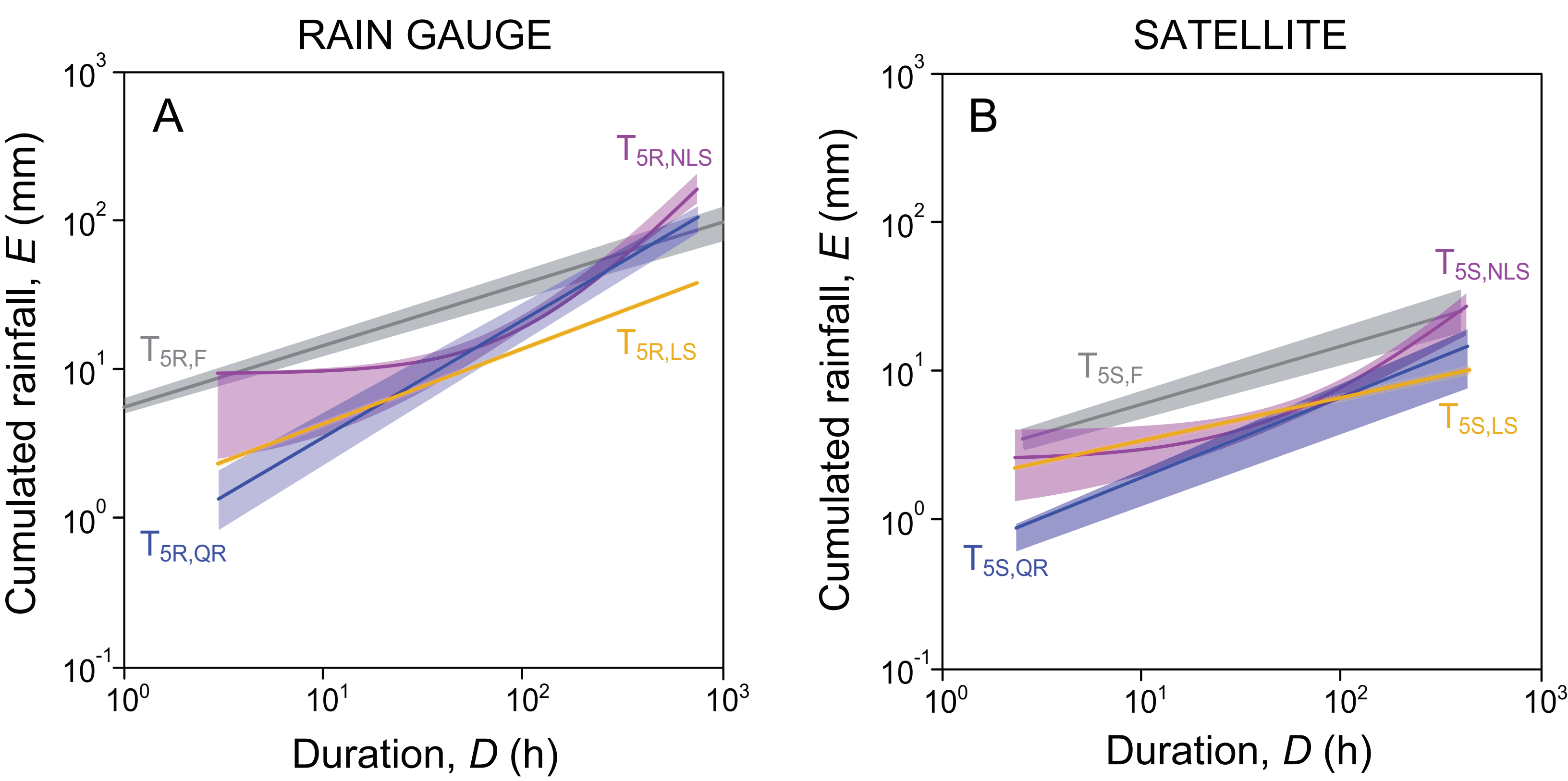

Figure 9 (Color)

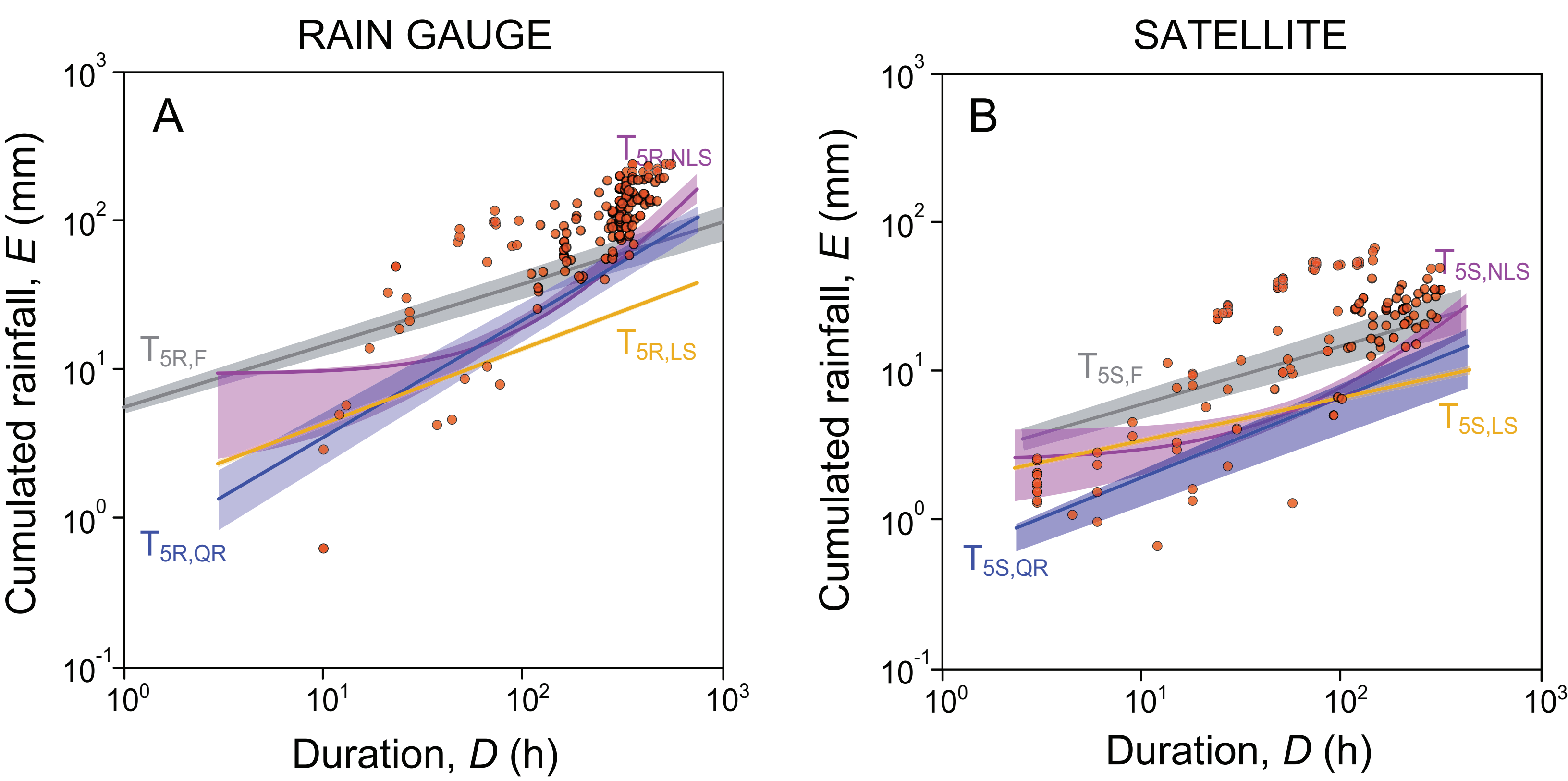

Figure 10 (Color)

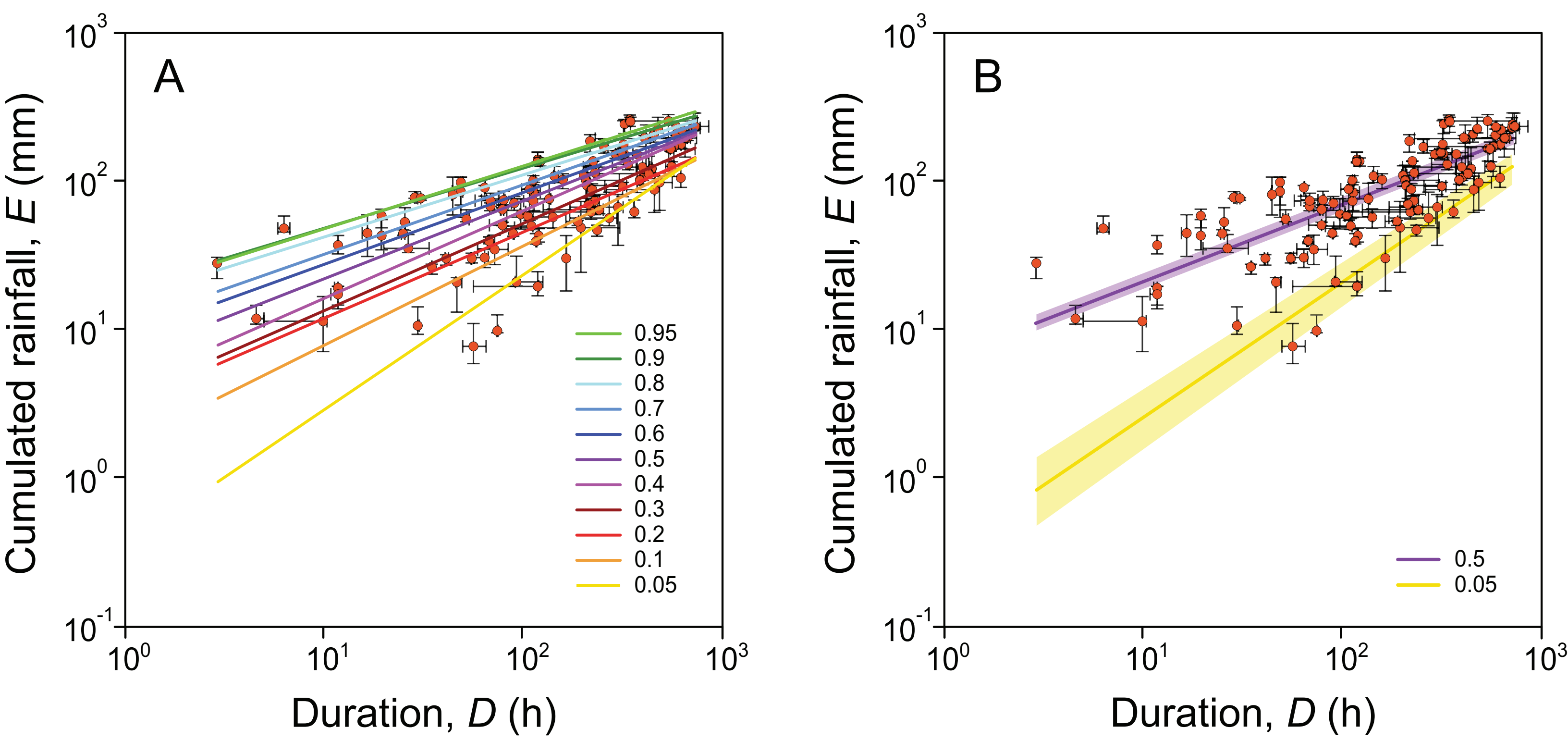

Figure 1 (Greyscale)

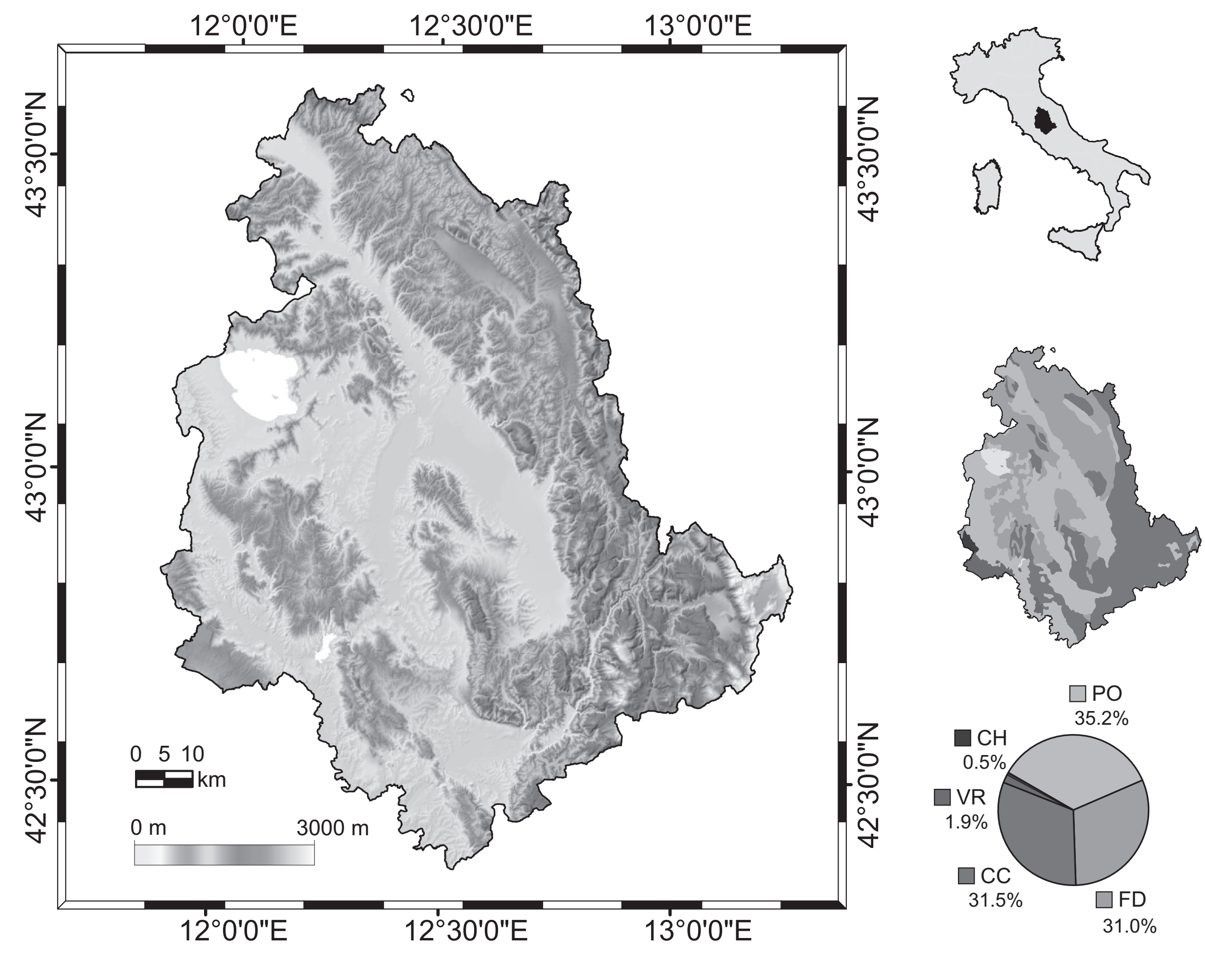

Figure 2 (Greyscale)

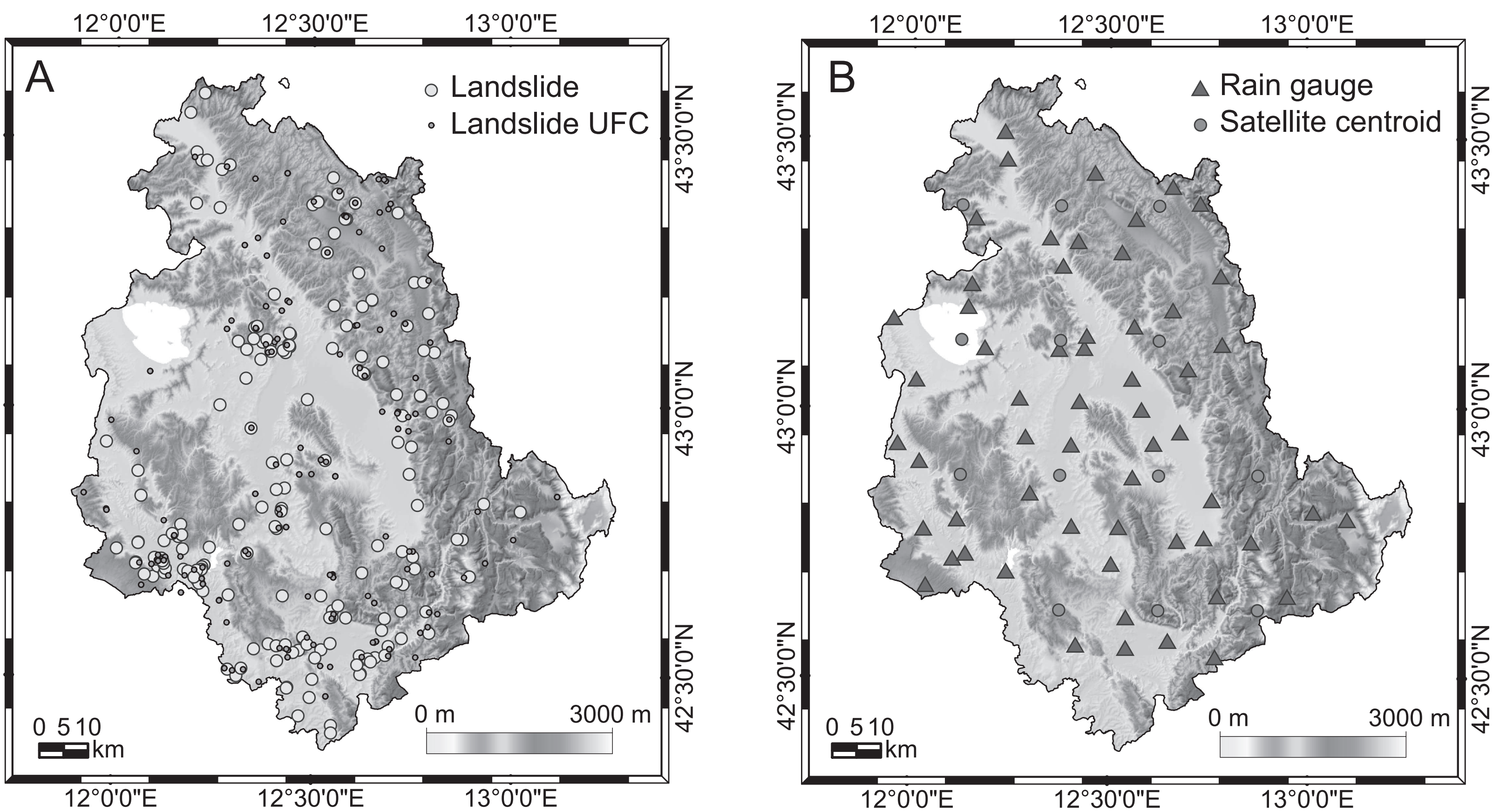

Figure 3 (Greyscale)

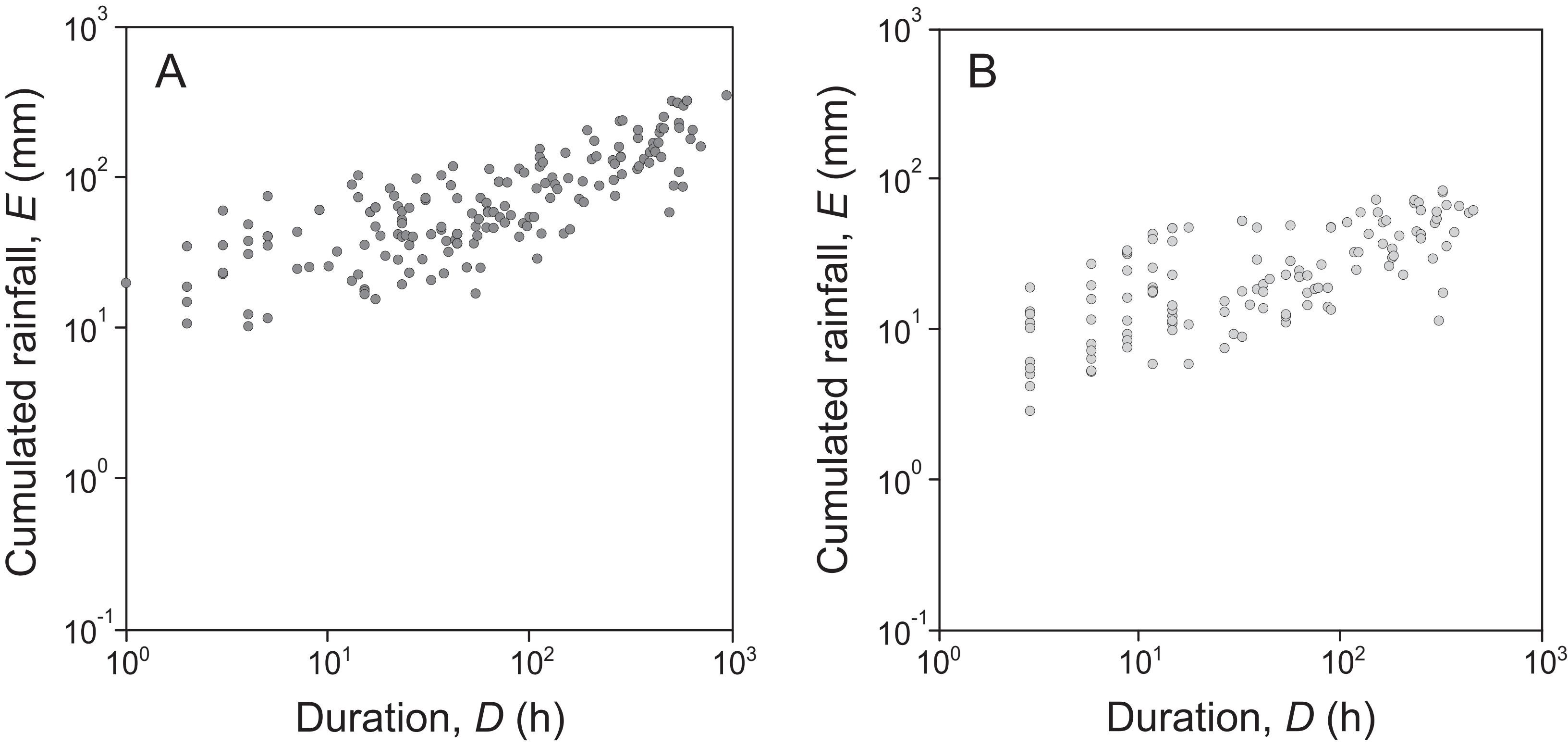

Figure 4 (Greyscale)

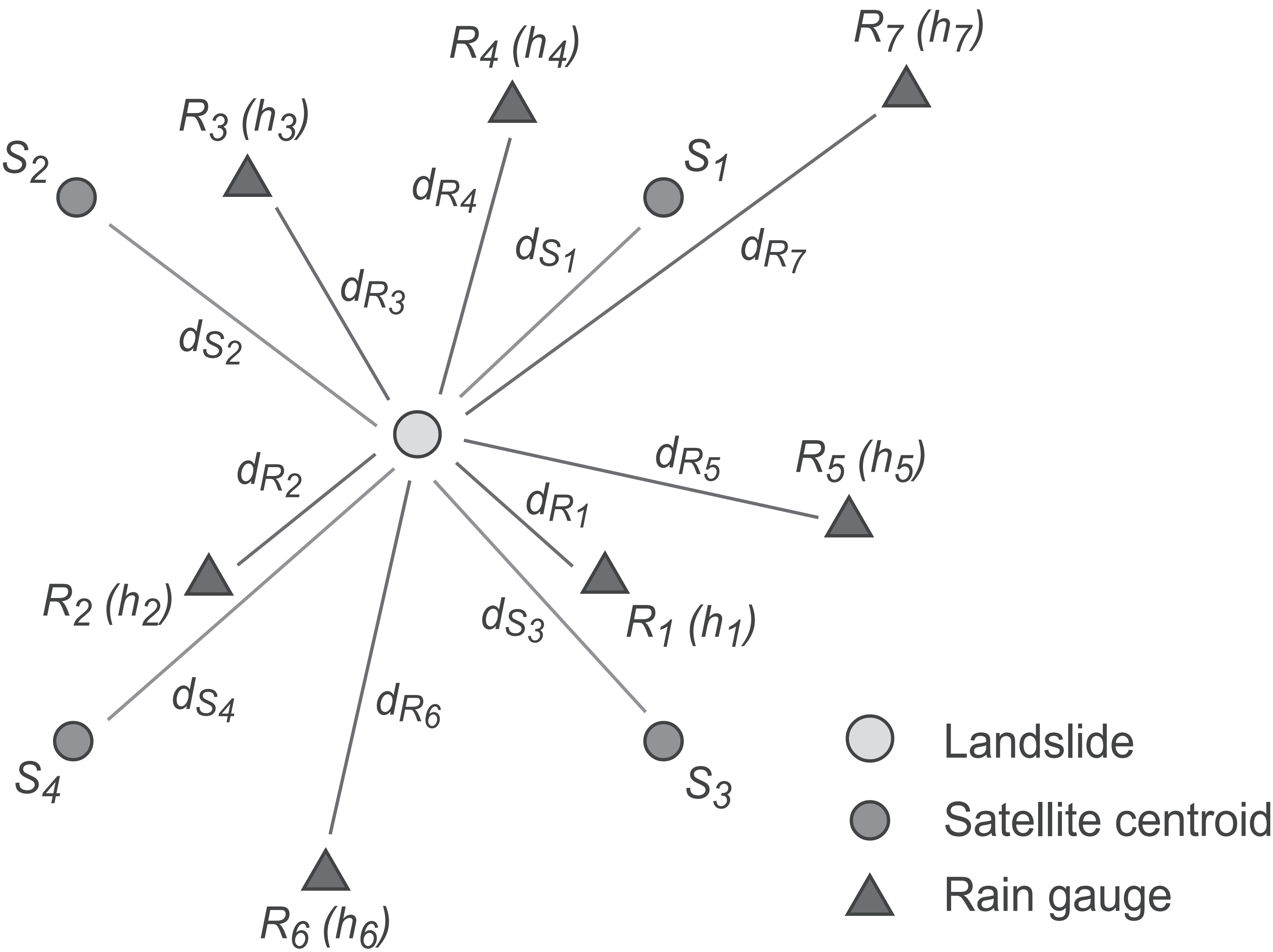

Figure 5 (Greyscale)

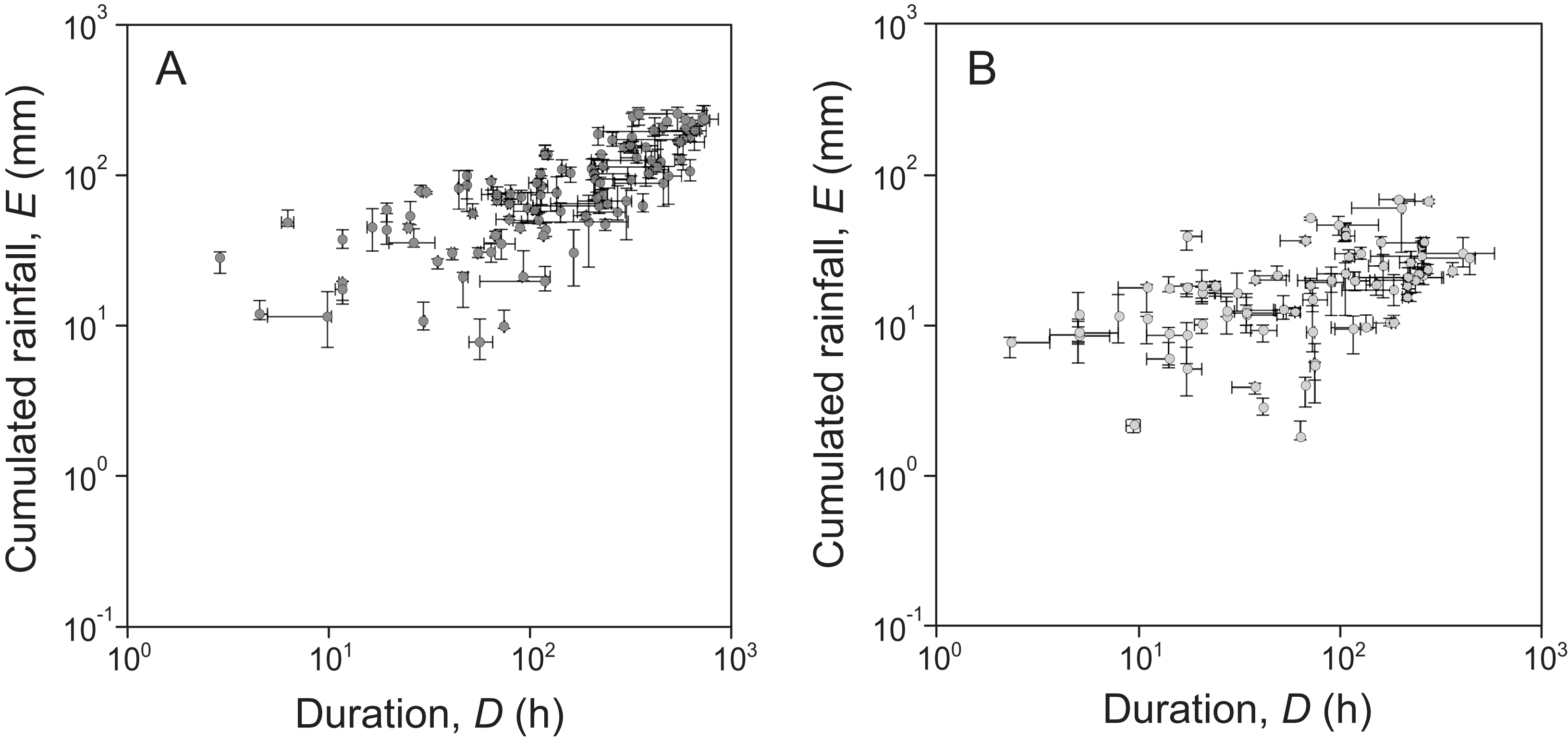

Figure 6 (Greyscale)

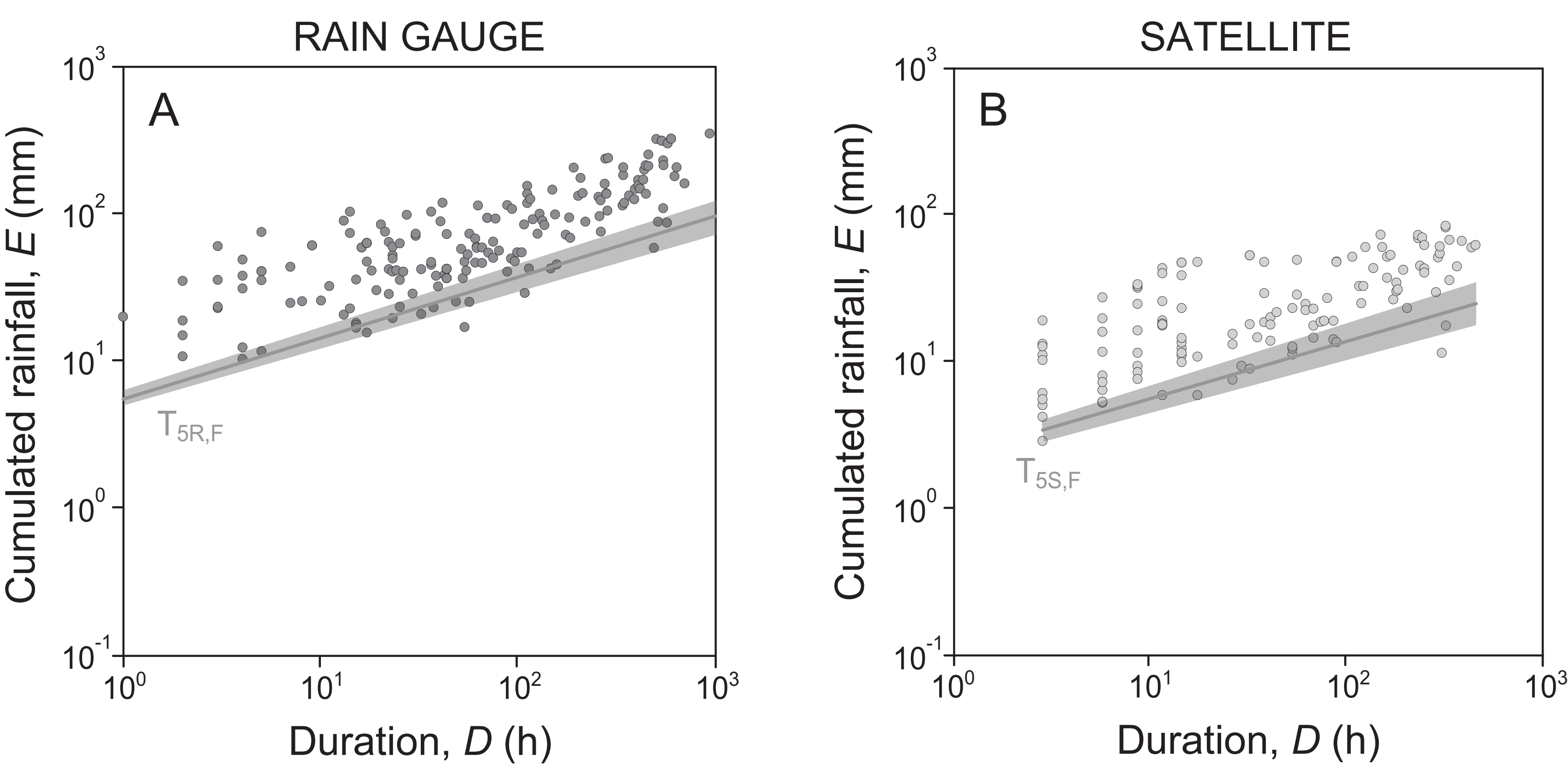

Figure 7 (Greyscale)

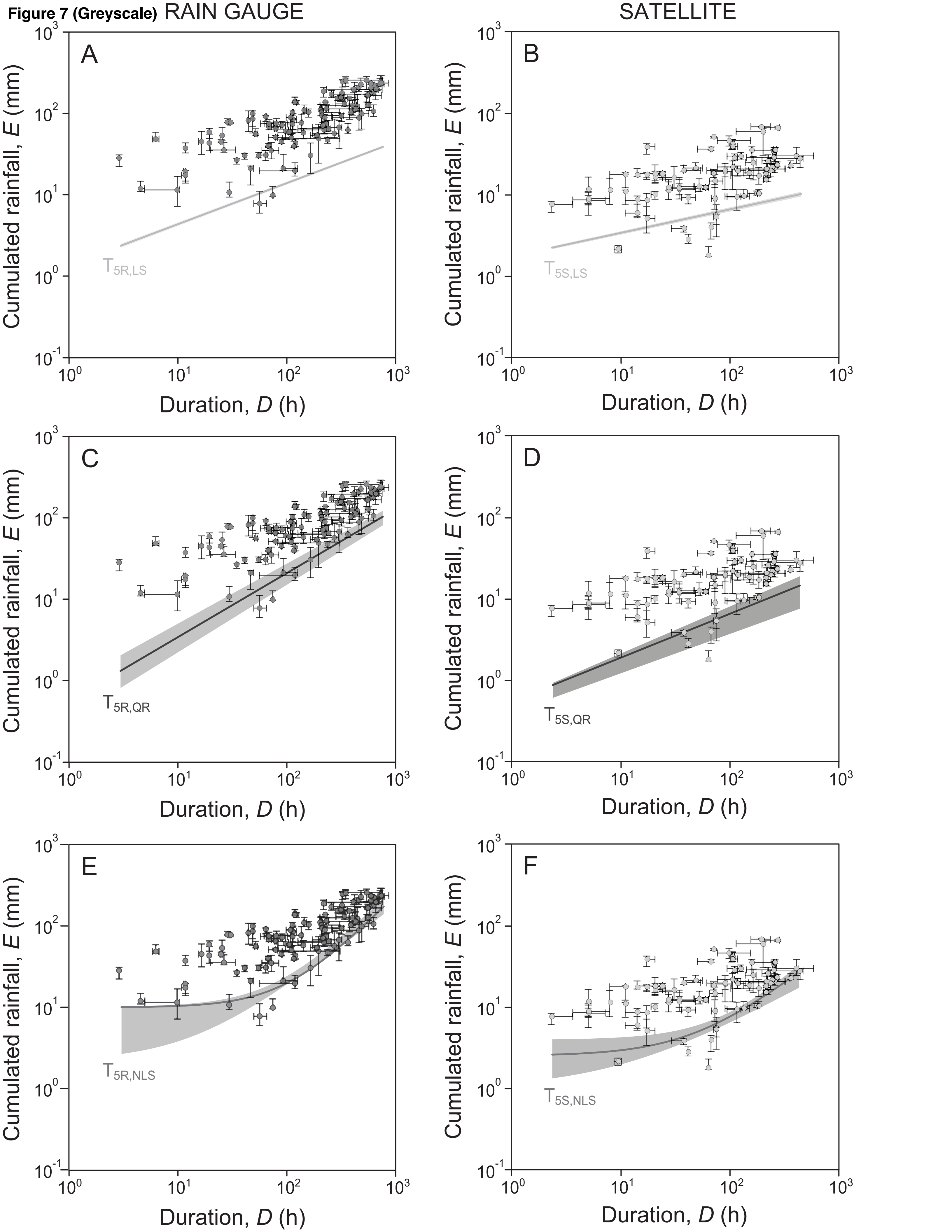

Figure 8 (Greyscale)

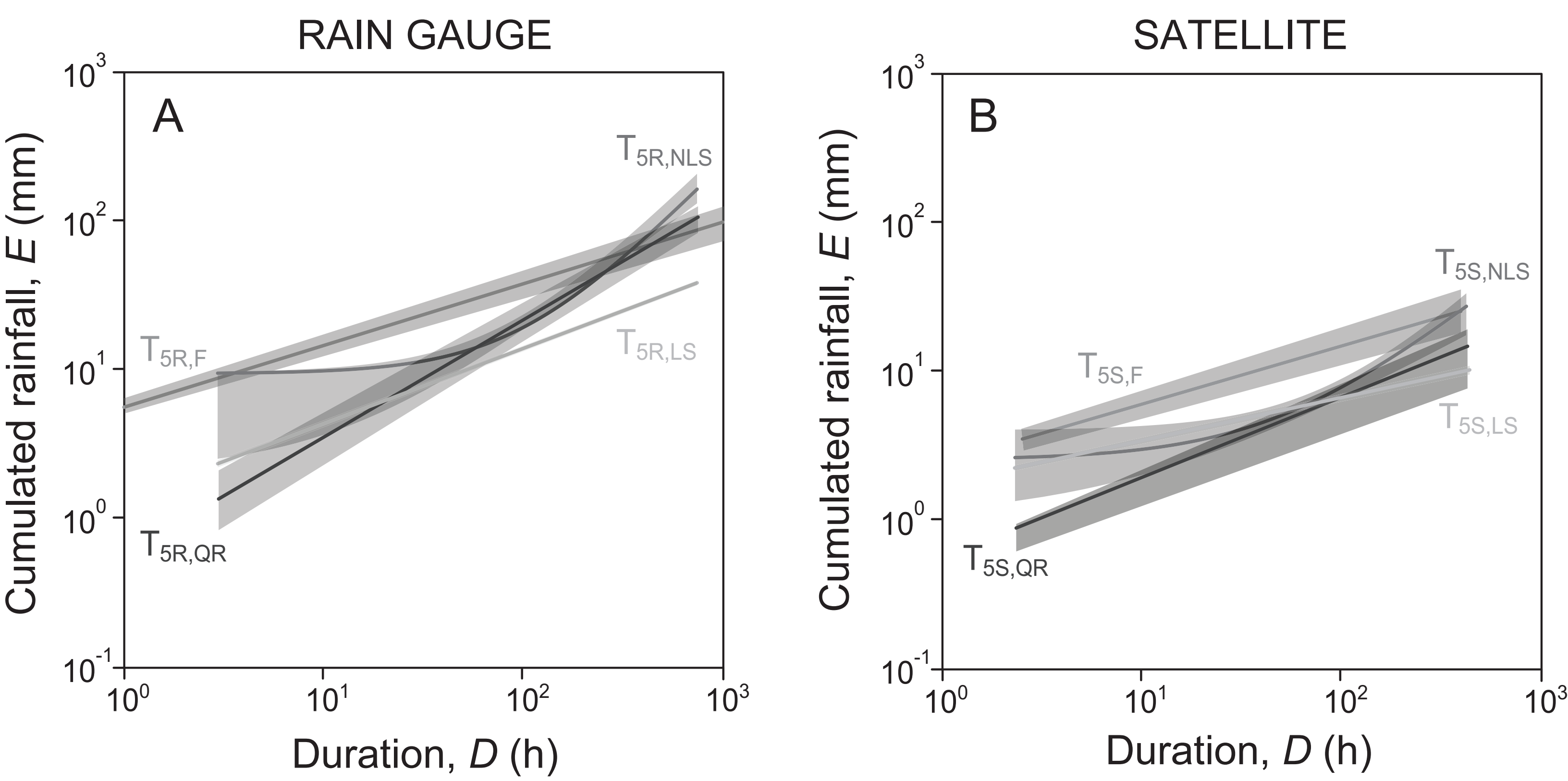

Figure 9 (Greyscale)

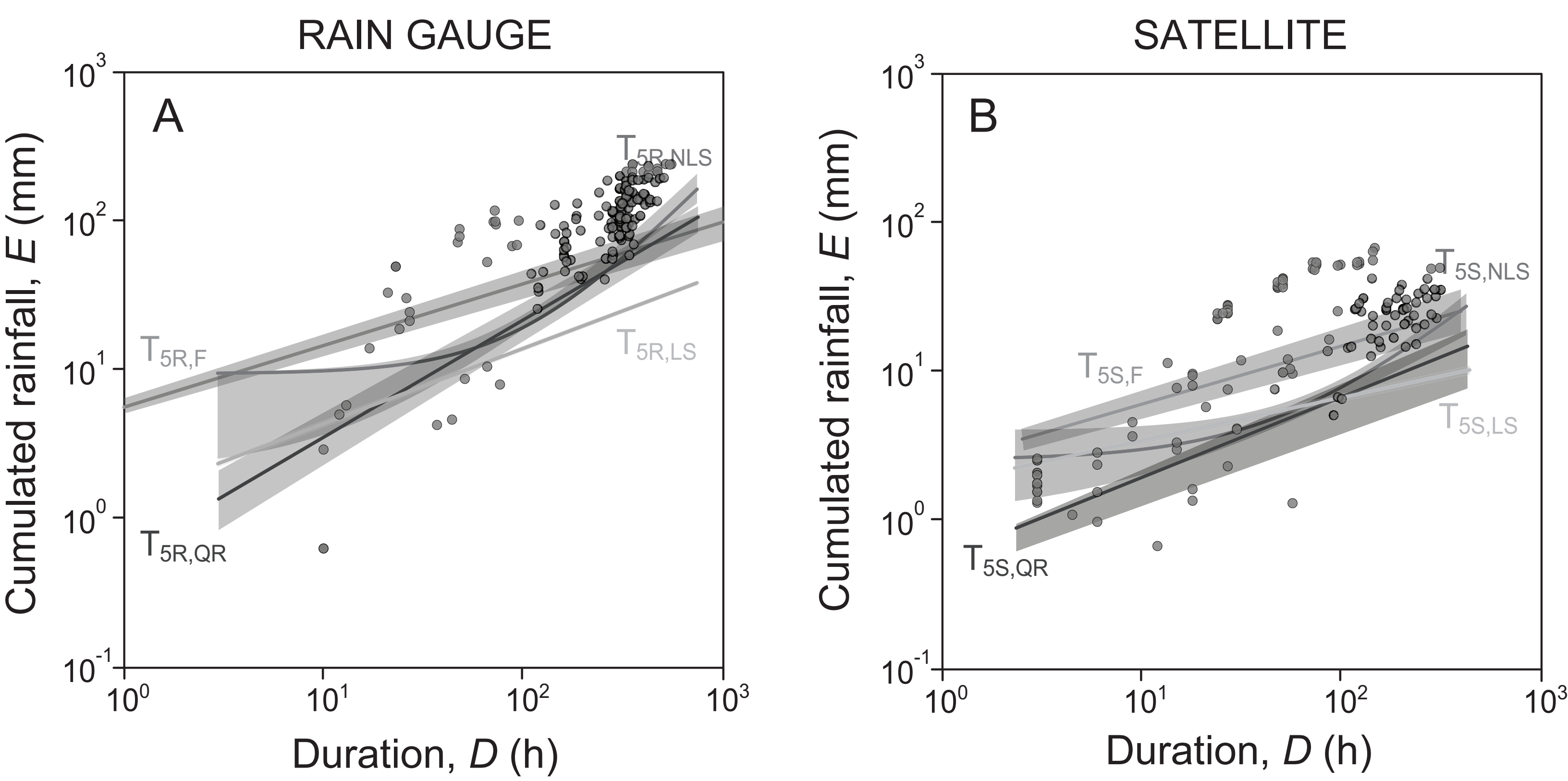

Figure 10 (Greyscale)